CORTEX 118 (2019) 165–187

Available online at www.sciencedirect.com

ScienceDirect

Journal homepage: www.elsevier.com/locate/cortex

Special issue: Research report

The hippocampus of birds in a view of evolutionary connectomics

Christina Herold [a,*], Philipp Schlömer [b], Isabelle Mafoppa-Fomat [b], Julia Mehlhorn [c], Katrin Amunts [a,b] and Markus Axer [b]

[a] C. & O. Vogt-Institute of Brain Research, Medical Faculty, Heinrich Heine University of Düsseldorf, Düsseldorf, Germany

[b] Institute of Neuroscience and Medicine INM-1, Research Center Jülich, Jülich, Germany

[c] Institute of Anatomy I, Heinrich Heine University of Düsseldorf, Düsseldorf, Germany

ARTICLE INFO

Article history:
Received 12 June 2018
Reviewed 30 July 2018
Revised 26 September 2018
Accepted 26 September 2018
Published online 11 October 2018

Keywords:
Adult neurogenesis
Doublecortin
Fiber tracking
3D polarized light imaging
Avian

ABSTRACT

The avian brain displays a different brain architecture compared to mammals. This has led the first pioneers of comparative neuroanatomy to wrong conclusions about bird brain evolution by assuming that the avian telencephalon is a hypertrophied striatum. Based on growing evidence from divers analysis demonstrating that most of the avian forebrain is pallial in nature, this view has substantially changed during the past decades. Further, birds show cognitive abilities comparable to or even exceeding those of some mammals, even without a "six-layered" cortex. Beside higher associative regions, most of these cognitive functions include the processing of information in the hippocampal formation (HF) that shares a homologue structure in birds and mammals. Here we show with 3D polarized light imaging (3D-PLI) that the HF of pigeons like the mammalian HF shows regional specializations along the anterior–posterior axis in connectivity. In addition, different levels of adult neurogenesis were observed in the subdivisions of the HF per se and in the most caudal regions pointing towards a functional specialization along the anterior–posterior axis. Taken together our results point to species specific morphologies but still conserved hippocampal characteristics of connectivity, cells and adult neurogenesis if compared to the mammalian situation. Here our data provides new aspects for the ongoing discussion on hippocampal evolution and mind.

1. Introduction

Understanding the routes of brain evolution in the context of cognition seems to be a challenging task for comparative neuroscientists following the fact that there are still many gaps to fill with a limited amount of species living in the 21st century. Nevertheless, in the past 50 decades researchers have presented data reporting that birds, cephalopods and even other taxa without a "six-layered" neocortex, show complex

* *Corresponding author*. C. & O. Vogt-Institute of Brain Research, Heinrich Heine University of Düsseldorf, 40225 Düsseldorf, Germany.
E-mail address: christina.herold@uni-duesseldorf.de (C. Herold).

https://doi.org/10.1016/j.cortex.2018.09.025

and intelligent behavior, tool use, social altruism and far more other skills comparable to or even exceeding those of some mammals (Güntürkün & Bugnyar, 2016; Karten, 2015). Together all of these cognitive functions and skills involve a functional cortical–basal ganglia circuit, which seemed to be highly conserved between species, like for example, the song system of birds and speech production in humans (Chakraborty & Jarvis, 2015; Karten, 2015). These findings however, have increased comparative studies and ongoing discussions dealing with the evolution of the "six-layered" neocortex (Bolhuis & Wynne, 2009; Butler, Reiner, & Karten, 2011; Gabi et al.., 2016; Güntürkün, 2005; Güntürkün, Ströckens, Scarf, & Colombo, 2017; Herculano-Houzel, Catania, Manger, & Kaas, 2015; Hevner, 2016; Kaas & Stepniewska, 2015; Montiel, Vasistha, Garcia-Moreno, & Molnar, 2016; Olkowicz et al., 2016; Shepherd & Rowe, 2017). In contrast, debates about hippocampal evolution are relatively tame (Striedter, 2016), although hippocampal (archicortical) structures evolved sometime in-between the paleo- and the neocortex, and many cognitive functions involve hippocampal circuits that are further integrated in the cortical–basal ganglia network. In addition, recent evidence emerged that it is likely that the "six-layered" neocortex has evolved from a common ancestor with a "three-layered" cortex, a morphology that is still present in hippocampal regions of different species (Güntürkün et al., 2017; Rowe & Shepherd, 2016; Shepherd & Rowe, 2017; Striedter, 2016; Ulinski, 1983). In our view, this observation makes the hippocampus an excellent candidate to study cortical evolution because the hippocampus shares a common origin in the amniote species (Medina & Abellan, 2009; Puelles, 2001, 2011) and many features of hippocampal functions are conserved, particularly spatial memory (Bingman & Muzio, 2017; Gagliardo, Ioale, & Bingman, 1999; Herold, Coppola, & Bingman, 2015; Witter, Kleven, & Kobro Flatmoen, 2017). Even more interesting, the hippocampal formation (HF) of birds displays a special morphology along its extension through the anterior–posterior axis. Most of it exhibits no clear three-layered laminar organization like the mammalian hippocampus or its homologue in the amniote species (Herold et al., 2014; Nomura & Hirata, 2017; Striedter, 2005, 2016). This variation however, raises the question what other properties of neurons or neuronal networks are required to serve conserved functions and what differences may exist and have evolved over more than 350 Million years of separate evolution in adaption to an ecologic niche (Fig. 1).

The HF in birds can be divided into several subdivisions, the V-complex, with its ventromedial (Vm), triangular (Tr) and ventrolateral (Vl) region, the dorsomedial region with its dorso-dorsomedial (DMd) and ventro-dorsomedial (DMv) subdivision and the dorsolateral region with its dorso-dorsolateral (DLd) and ventro-dorsolateral (DLv) subdivision (Fig. 2; Herold et al., 2014). Despite the differences in the overall architecture, cell types and connections of the HF in birds show many similarities to those of mammals (Atoji, Wild, Yamamoto, & Suzuki, 2002; Casini, Bingman, & Bagnoli, 1986; Colombo & Broadbent, 2000; Hough, Pang, & Bingman, 2002; Krebs, Erichsen, & Bingman, 1991; MacPhail, 2002; Sherry, Grella, Guigueno, White, & Marrone, 2017). However, there is an ongoing discussion, which subdivisions

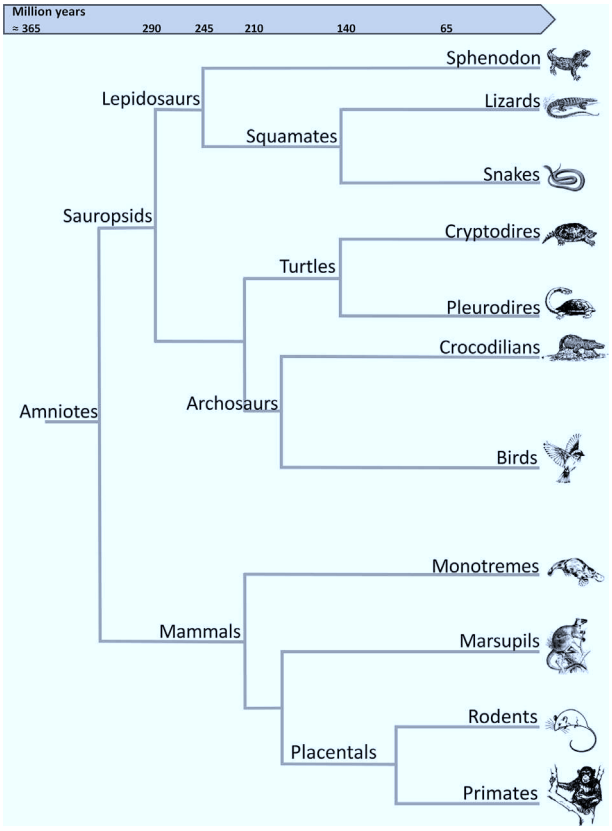

Fig. 1 – Simplified phylogenetic tree of amniotes. Analysis of single cell transcriptomics support the idea that the anlage of the hippocampal formation, i.e., dentate gyrus and cornu ammonis was already present in the ancestor of all amniotes (Tosches et al., 2018). Since then, several million years of separate evolution occurred between birds and mammals.

of the HF in birds correspond to their mammalian counterparts, i.e., the dentate gyrus (DG), the cornu ammonis (CA) fields, the subiculum and the entorhinal cortex (Abellan, Desfilis, & Medina, 2014; Atoji, Sarkar, & Wild, 2016; Herold et al., 2015; Medina, Abellán, & Desfilis, 2017). New theories of the evolution of DG as a late evolving structure and an exclusive addition to the hippocampus of mammals have further questioned whether a DG as strict as in mammals even exists in birds or not (Atoji et al., 2016; Bingman & Muzio, 2017; Bingman, Rodriguez, & Salas, 2017; Kempermann, 2012; Striedter, 2016). However, recent findings by analysis of single-cell transcriptomics of the reptilian medial most cortex, particularly the dorsomedial cortex, support the hypothesis that the hippocampal regions, including DG, CA1 and CA3 were already present in the ancestor of all amniotes (Tosches et al., 2018).

Yet, another clue comes from new insights of functionally different domains in the mammalian hippocampus. Based on genetic and connectional data the hippocampus of mammals can be compartmentalized into multiple domains along the longitudinal/dorsal-ventral axis (Dong, Swanson, Chen, Fanselow, & Toga, 2009; Ohara, Sato, Tsutsui, Witter, & Iijima, 2013; Thompson et al., 2008; Witter et al.,

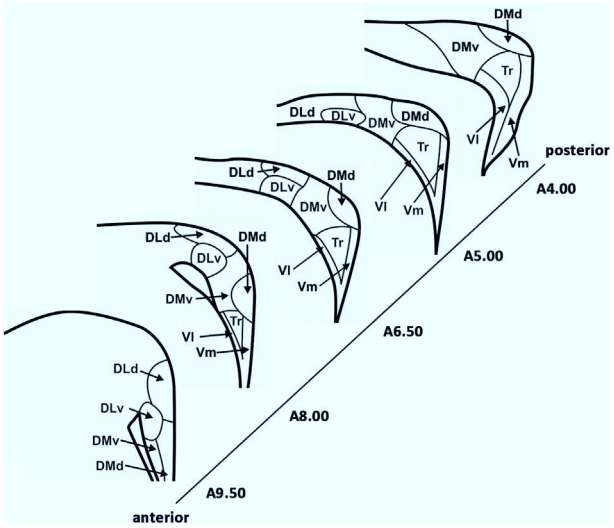

Fig. 2 – The hippocampal formation of the pigeon. Schematic outlines along the anterior–posterior axis according to Herold et al. (2014). Atlas levels referring to Karten and Hodos (1967, p. 195). The major subdivisions are the V-region comprising the lateral (Vl) and medial (Vm) layers and the triangular area in between (Tr), the dorsomedial region with its dorsal (DMd) and ventral (DMv) subdifferentiation, and the dorsolateral region (DL) including the further subdivisions dorsal (DLd) and ventral (DLv).

2017). Further, a large body of connectional and functional data, including adult neurogenesis in rodents and primates, revealed that the dorsal hippocampus (septal pole or posterior in primates) is involved in spatial memory and navigation, and showed higher levels of adult neurogenesis, while the ventral hippocampus (temporal pole or anterior in primates) mediates emotion, anxiety, stress-related behavior and cognitive flexibility, and exhibits lower levels of adult neurogenesis (Anacker & Hen, 2017; Colombo, Fernandez, Nakamura, & Gross, 1998; Fanselow & Dong, 2010; Strange, Witter, Lein, & Moser, 2014; Witter et al., 2017). This functional differentiation in case of stress-related behavior might also exist in the avian HF (Robertson et al., 2017; Smulders, 2017).

Up to now, only a few researchers have explored the rostro-caudal axis in the avian HF (Fig. 2) and less is known about the basis of functional differences along the axis. Therefore, we decided to analyze two different components of hippocampal functional circuity. First, we will present data for the homing pigeon (*Columba livia f.d.*) with a focus on rostro-caudal differences in hippocampal connectivity at the microscale level by using the newly developed method of 3D-polarized light imaging (3D-PLI). 3D-PLI has been shown to be a powerful tool to analyze fiber architecture, and the course of fibers and fiber tracts in mammals (Axer, Amunts, et al., 2011; Axer, Gräßel et al., 2011; Zeineh et al., 2017; Zilles et al., 2016). Second, we will present data of neurogenic markers for adult neurogenesis in the pigeon rostro-caudal axis of the HF.

2. Material and methods

2.1. Animals

In total, we examined eleven adult homing pigeon brains (*C. livia f.d.*) of the same age originating from our local breeding colony, which were raised in the same loft (250 cm × 190 cm × 190 cm) and lived there under identical conditions. The pigeons were allowed to fly freely and food, grit and water were provided ad libitum. All experimental procedures were approved by the national authority (LANUV NRW, Germany) and were carried out in accordance with the National Institute of Health Guide for Care and Use of Laboratory Animals.

2.2. 3D-polarized light imaging

2.2.1. Tissue-processing

Animals for the Polarized Light Imaging (n = 2) were euthanized with Pentobarbital (70 mg/kg), decapitated, brains were removed from the skull, and immediately fixed in 4% buffered formalin pH 7 and stored at 4 °C. Two weeks later brains were transferred into a solution of 10% Glycerin, 2% DMSO and 4% formalin pH 7 for five days, and subsequently transferred into a solution of 20% Glycerin, 2% DMSO and 4% formalin pH 7 for additional two weeks. Brains were frozen and stored at −80 °C. They were cut in serial coronal or sagittal 60 μm sections with a cryostat microtome (Leica Biosystems, Nussloch Germany). Slices were thaw mounted on un-gelatinized slides, freeze dried and coated in 20% Glycerin three days before the 3D-PLI measurements started. After the measurements, slices were further processed for Nissl staining with Cresyl violet.

2.2.2. Imaging

In order to make the fiber architecture of brain tissue visible, linearly polarized light has been applied to the histological sections and the light transmission has been sampled at 9 or 18 vertical polarization planes covering 180° by means of a circular analyzer (Axer, Amunts, et al., 2011; Axer, Gräßel et al., 2011). The interaction of polarized light with the birefringent components of the nerve tissue, i.e., the myelin, allows for the extraction of predominating fiber orientations in tiny volumes of 1.3 μm × 1.3 μm × 60 μm.

The polarimetric setup is based on a standard bright field microscope (with Köhler illumination) with two polarizing filters and a movable specimen stage (Märzhäuser Wetzlar, Germany) introduced into the beam path (Fig. 3). The wavelength spectrum (550 ± 5 nm) has been adapted to the polarizing filter specifications by means of a white light LED in combination with a narrowband pass filter next in line. The size of the square field of view of the monochrome CCD camera (QImaging Retiga 4000R) is 2.7 × 2.7 mm^2 providing a pixel resolution of 1.3 microns. The transmission intensity of the whole specimen is imaged with a tile overlap of 1.0 mm at 18 vertical polarization plane angles (ρ) for the frontal sections and with a tile overlap of .75 mm at 9 vertical polarization angles for the sagittal sections respectively, in order to determine accurately the predominant fiber orientation in each of 1.3 μm × 1.3 μm × 60 μm voxel (Fig. 4f).

Using the Jones calculus for flat polarization optics (Jones, 1941) three modalities can be derived from the sinusoidal dependence (Fig. 4e) of the transmission intensity I on the polarization plane angle (ρ):

$$I(\rho) = \frac{Transmittance}{2} \cdot [1 + \sin(2\rho - 2 \cdot Direction) \cdot Retardation]$$

$$Retardation = \sin\left(2\pi \cdot \frac{Section\ Thickness}{Light\ WaveLength} \cdot Birefringence \cdot \cos^2(Inclination)\right)$$

Transmittance (arbitrary units) is the mean intensity of the light transmission through the tissue (Fig. 4a). *Retardation* (0–1) is the vertical projection of the cumulative tissue birefringence normalized by the transmittance at a given light wavelength (Fig. 4b). *Direction* (0°–180°) is the predominant in-plane nerve fiber orientation (Fig. 4c).

The out-of-plane elevation angle of the nerve fiber is called *Inclination* (Fig. 4d) and can be estimated from retardation and transmittance by means of four parameters determined on the basis of their gray value distributions over the whole section:

1) *retmaxwm*: maximum retardation of the white matter 2) *retmaxgm*: maximum retardation of the gray matter 3) *tmaxgm*: maximum transmittance of the gray matter 4) *tmeanwm*: mean transmittance of the white matter (Reckfort, 2015). The parameter *retmaxgm* has been introduced in addition to account for the weak influence of the gray matter retardation. These four parameters approximately determine the relation between the retardation and the inclination by means of the transmittance:

$$\frac{\sin^{-1}(Retardation)}{\cos^2(Inclination)} = \frac{log\left(\frac{tmaxgm}{tmeanwm}\right)}{\log\left(\frac{tmaxgm}{Transmittance}\right) \cdot \sin^{-1}\left(retmaxwm + (retmaxgm - retmaxwm) \cdot \frac{Transmittance - tmeanwm}{tmaxgm - tmeanwm}\right)}$$

Due to the presence of artificial inhomogeneity in the transmittance induced by glycerol at variable time delays between tissue embedding and 3D-PLI-measurement, these parameters had to be slightly adapted subsequently to avoid the saturation of the inclination at 0° or 90° degrees in areas prone to this artifact like deep white matter or scarcely myelinated nuclei. The inclination values are compromised by this modification to the point of about +5 up to +10°.

2.2.3. Fiber orientation maps

Direction, inclination and mask provide a full set of polar coordinates for the calculation of a 3D-vector array of fiber orientations. The vector data of a single section provided by 3D-PLI are represented by color images called fiber orientation maps (FOMs). A point on the colored surface of a hemisphere represents the color of a corresponding 3D fiber orientation (Fig. 4f). Yet a quarter sphere is sufficient because flat 3D-PLI without tilting the light beam does neither differentiate forward and backward orientation nor the sign of the fiber inclination (downward or upward). The hue corresponds to the direction of the in-plane projection of the fiber orientation.

The fiber inclination on the other hand is coded by saturation and brightness (Fig. 4g). In case of the RGB-color-code (Fig. 5A) hemisphere fiber orientations are reflected by colors only. The principal directions (left–right, up–down, front–rear) are corresponding to the fundamental colors (red, green, blue). In the HSV-color-code (Fig. 5B) hemisphere fiber orientations are reflected by hue, saturation and brightness. In the HSV-black version the brightness decreases with increasing inclination staining the poles at 90° black.

The reference for a single vector representation is generally not a single fiber but all birefringent tissue compartments inside a volume element (voxel) contributing to an image pixel. There are two reasons for signal loss in the white matter: fiber crossings and steep fibers with inclinations nearby 90°. Therefore, in areas of massive fiber intermingling at scales below the section thickness of 60 microns the direct representation of the fiber orientation by color and saturation is replaced by an extinction texture. Hence fibers stay visible in the FOM, however, orientation values are getting lost (Fig. 5C).

2.3. Immunohistochemistry

Animals used for immunohistochemistry of adult neurogenesis markers (n = 9, female 5, male 4, all age-matched) were injected i.m. on three consecutive days with BrdU (50 mg/kg). Twelve weeks after the injections animals were deeply anesthetized with Pentobarbital (70 mg/kg), transcardially perfused with 4% paraformaldehyde and brains were removed. After 2 h of postfixation (4% paraformaldehyde + 30% sucrose) and 24 h of cryoprotection (30% sucrose in phosphate buffer), the brains were frozen and cut in serial coronal 40 μm sections with a microtome (Leica Biosystems, Nussloch, Germany).

Coronal sections from one series out of 10 of the whole pigeon brain were immunohistochemically processed for 1) fluorescent double-labeling detection of DCX (anti-DCX ab18723, abcam, USA, see Fig. 6A and B) and BrdU (anti-BrdU OBT0030, AbD serotec, USA), or 2) triple fluorescent labeling

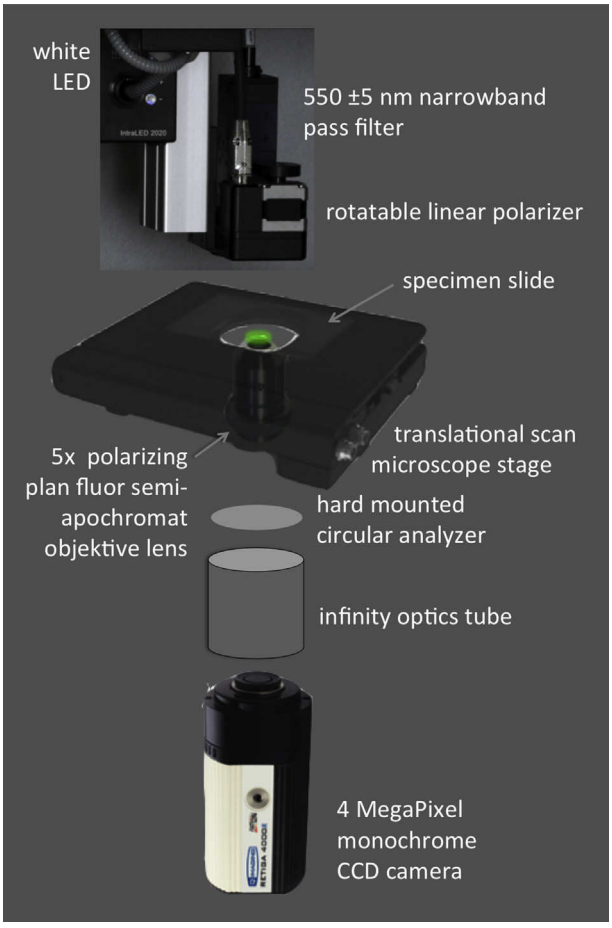

Fig. 3 – Hardware setup of the polarization microscope.

detection of BrdU (anti-BrdU OBT0030, AbD serotec, USA), NeuN (anti-NeuN MAB377, Millipore, Germany) and GFAP (ab16997, abcam, USA, see Fig. 6C and D).

1) Briefly, free-floating sections were rinsed 2 times in phosphate buffered saline (PBS). Subsequently slices were incubated in 2 N HCl at 45 °C for 30 min and .1 M borate buffer pH 8.5 for 10 min. Sections were than washed in PBS for 10 min that was followed by a blocking step with 3% goat serum (Vector, USA) in PBS + Triton-X .3% (PBS-T) for 60 min. This was followed by incubation with a primary antibody mix anti-BrdU (1:200) and anti-DCX (1:500) overnight at 4 °C. After that sections were washed 3 times in PBS that was followed by incubation with the secondary antibody mix containing goat anti-rat Alexa 488 (1:200) and goat anti-rabbit CY3 (1:500; both Jackson-Immuno Research, USA) for 2 h at darkness. At all further steps, sections were handled at a minimum of light or in complete darkness. After incubation sections were washed 3 times with PBS and 2 times with PB, mounted on gelatin-coated glass slides, air-dried for 24 h and then dipped into distilled water and directly coverslipped with Fluoromount-G (Southern Biotec, USA). The slides were than taken to a fluorescent microscope system AxioScan.Z1 (Zeiss, Germany) and the whole sections were scanned for digitalization of photomicrographs at 20× magnification. All sections were analyzed with the software Zen2 (Zeiss, Germany), by delineation of ROIs (i.e., subdivisions of the HF) and counting immunereactive cells with the counting tool so that a value for each region of the number of immunoreactive cells (either BrdU, or DCX)/area (mm^2) was determined.
2) To detect BrdU+ cells, sections were treated like in the labeling procedure of 1). After the pre-processing, sections were incubated with the primary antibody mix anti-BrdU (1:200), anti-NeuN (1:1000) and anti-GFAP (1:500)

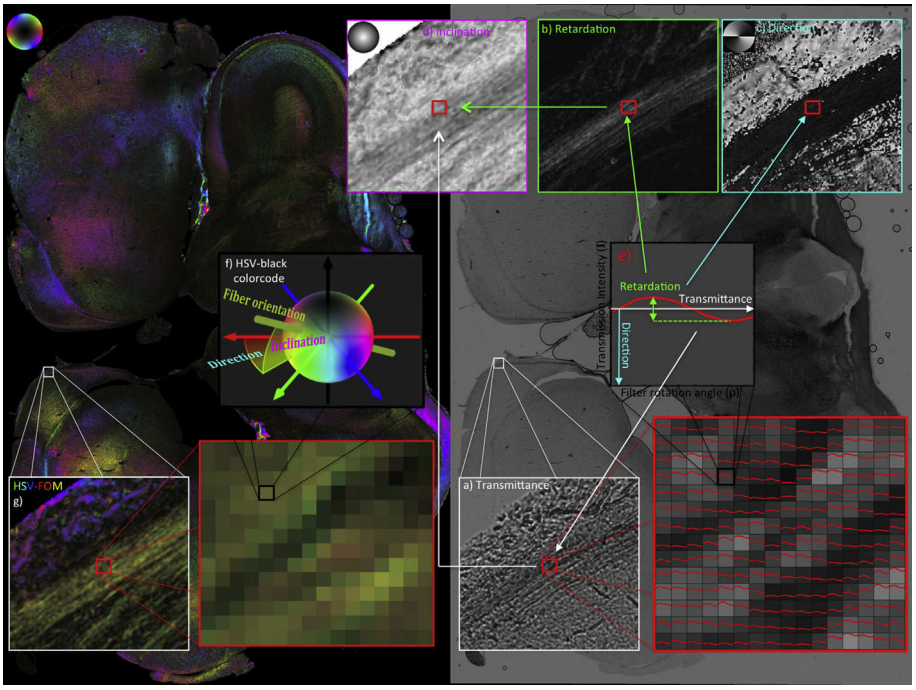

Fig. 4 – Data processing pipeline of 3D-PLI (a–f). For details see section 2.2.2 and 2.2.3 in the material and methods section.

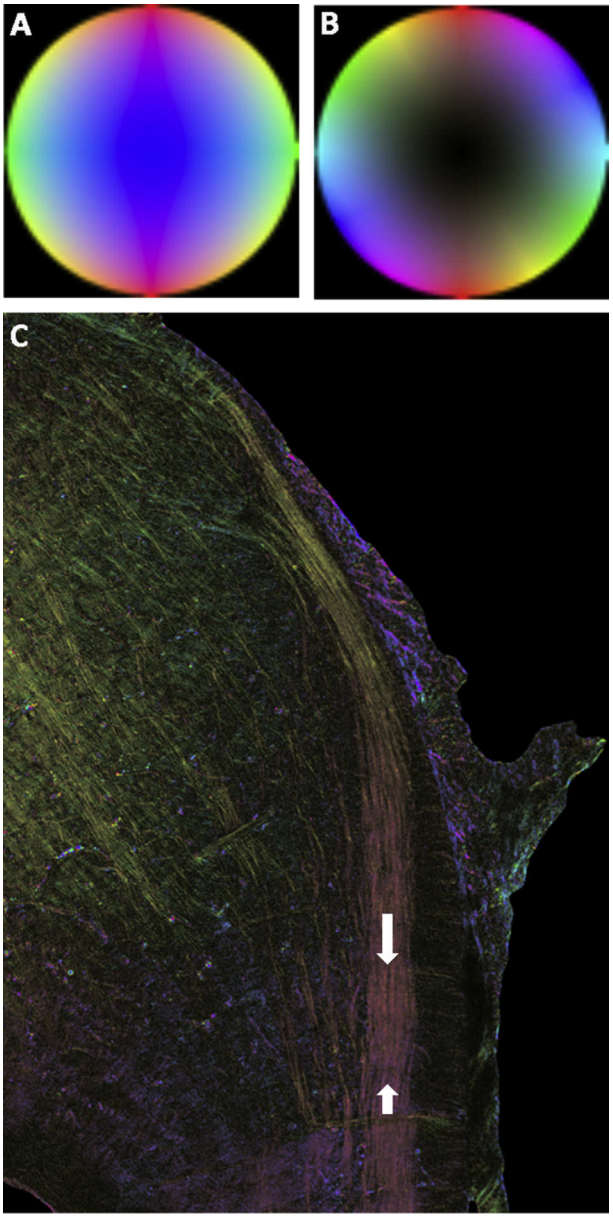

Fig. 5 – FOM color-codes and signal extinction. A: RGB color code. B: HSV-black color code. C: Signal extinction on the HSV-black map (white arrows) of radial fibers near the interhemispheric fissure crossing the septal tract in the medial part of the hippocampal formation.

overnight at 4 °C, washed (3× PBS), and then incubated with the secondary antibody mix containing donkey anti-mouse Alexa 647 (1:200; Dianova, Germany) goat anti-rabbit FITC (1:200; Cayman Chemical, USA) and goat anti-rat CY3 (1:200; Millipore, Germany) for 2 h at darkness. All further steps were identical to the labeling procedure of 1).

All antibodies were validated by Western-blotting procedures or showed specific binding in previous studies (Fig. 5E; Melleu, Santos, Lino-de-Oliveira, & Marino-Neto, 2013; Robertson et al., 2017). Tissue samples were lysed at 4 °C with 50 mM Tris–HCL buffer (pH 7.4) containing 1% IGEPAL, 150 mM NaCl, 1 mM ethylenediaminetetraacetic acid, .1% SDS, 1 mM dithiothreitol and 2% glycerin. After homogenization, the lysates were centrifuged at 20.000 *g* at 4 °C. For sodium dodecyl sulfate polyacrylamide gel electrophoresis (SDS-Page) and Western Blot analysis, the supernatant was added 1:4 to a 4× gel loading buffer containing 1.25% mercaptoethanol (pH 6.8) and heated to 95 °C for five minutes. The probes were subject to gel electrophoresis (12%) using .3 μg protein per lane. Proteins were transferred to nitrocellulose membranes using a dry transfer apparatus (Invitrogen, Carlsbad, USA). Blots were blocked for 1 h with a blocking solution containing bovine serum albumin solubilized in 20 mM Tris–HCL pH 7.6, 150 mM NaCl and .1% Tween 20, and incubated overnight with the primary antibody (see list above) at 4 °C. After several rinsing steps and incubation with horseradish peroxidase-coupled immunoglobulin G, anti-rabbit IgG or anti-mouse IgG (both Jackson-Immuno Research, USA) at room temperature for 1 h, blots were washed and developed by using enhanced chemiluminescent detection (BioRad).

2.4. *Data analysis*

At a first step, the atlas levels (Karten & Hodos, 1967, p. 195) of the brain sections from pigeons for 3D-PLI and immunohistochemistry measurements were determined.

For analysis of the 3D-PLI data, visual analyses of frontal and sagittal sections enabled us to take advantage of the extremely high in-plane resolution of 3D-PLI to optimally detect the dorsal–ventral and medial–lateral trajectories in the frontal images, and dorsal–ventral and anterior–posterior trajectories in the sagittal images. We identified the orientation of fibers by examining the color-coded fiber orientation maps, examining the color as well as the image texture (e.g., numerous lines pointing in one direction). Dark regions on transmittance images that were not cell bodies were generally considered to represent myelin. 3D-PLI is maximally sensitive for fibers oriented in-plane; on frontal section images, fibers oriented through-plane (i.e., along the anterior–posterior axis of the hippocampus formation) would appear dark on the transmittance images, but show reduced or no color orientation. Therefore, the sagittal images were used to confirm through-plane orientation of pathways. Further anterior–posterior long-range connections were first analyzed and identified in the sagittal sections, and then combined with the analysis of the frontal sections.

Combining the results of 3D-PLI with our subregion segmentation, we identified the major pathways according to known connectivity patterns from earlier avian studies (see Atoji & Wild, 2006; Shanahan, Bingman, Shimizu, Wild, & Güntürkün, 2013 for review), and compared it with the PLI data. A known limitation of 3D-PLI fiber tracking, however, is that we cannot determine, whether a fiber, or a fiber bundle, is entering or leaving the HF, so we used earlier results of tracing studies to guide the interpretation.

For immunohistochemistry, data of the hippocampal subregions defined by Herold et al. (2014) from atlas levels A 10.25 (anterior) to A 3.75 (posterior) were analyzed. The number of immunoreactive cells (BrdU+, DCX+, BrdU+/NeuN+, BrdU+/GFAP+)/area (mm^2) was averaged for the following coordinates ±500 μm: A 4.25, A 5.50, A 6.75, A 8.25 and A 9.50.

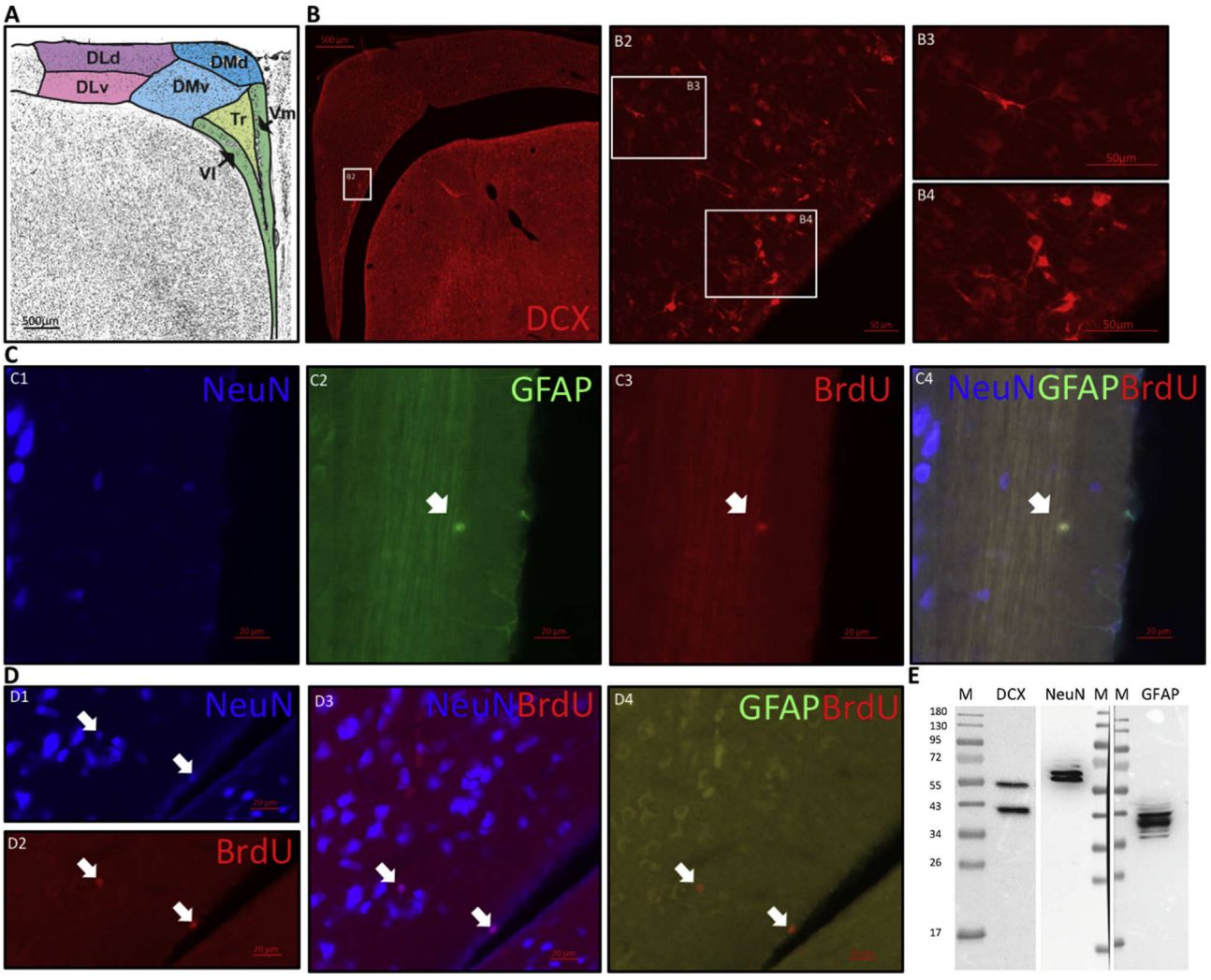

Fig. 6 – Expression of neurogenic markers in the hippocampal formation of the pigeon. A: Different subdivisions of the hippocampal formation. B: DCX expression in the hippocampal formation (B1–2) and different DCX-ir cell types characterized by shape, the ovoid cells (B3) and the triangular cells (B4) in the V-region. C: NeuN (C1), GFAP (C2), BrdU (C3) triple labeling in Vm showing double labeled BrdU/GFAP cells (C4). D: NeuN (D1), GFAP, BrdU (D2) triple labeling in Vl showing double labeled BrdU/NeuN cells (D3) excluding GFAP labeling (D4). E: Western-Blots validating the antibodies for DCX, NeuN and GFAP showing the expected bands between 55–40 kDa (DCX), 72–55 kDa (NeuN) and 43–34 kDa (GFAP). Abbreviations see text.

To determine differences in BrdU+, DCX+, BrdU+/NeuN+, BrdU+/GFAP+ cells among the HF at different anterior–posterior levels or across subdivisions, we first applied a Friedman ANOVA for each tested neurogenic marker or marker pair. If significant, pair-wise comparisons were run with the Wilcoxon-rank test. For the general statistical analyses, Statistica 13 (StatSoft, Tulsa, USA) was used. The significance level was set at .05.

3. Results

3.1. *Connectivity of the pigeon hippocampal formation along the anterior–posterior axis*

Along the anterior–posterior axis, the pigeon HF is moving from a rostro-medial to a caudo-lateral position in the dorsal forebrain (Fig. 2). We generally confirmed earlier tracing studies showing that the pigeon HF is connected to the lateral and medial septum (SL and SM), the nucleus taeniae of the amygdala (TnA), the lateral part of the bed nucleus of the stria terminalis lateralis (BSTL), the nucleus of the diagonal band (NDB), the hypothalamus, i.e., the nucleus periventricularis magnocellularis (PVM), the dorsolateral corticoid area (CDL), the hyperpallium apicale (HA) and laterale (HL), the cortex piriformis (CPi), the arcopallium ventrale (AV) and intermediale (AI) and inter-hippocampally via commissural fibers through the commissura pallii (CPa; Atoji, Saito, & Wild, 2006; Atoji & Wild, 2004; Atoji et al., 2002; Benowitz & Karten, 1976; Casini et al., 1986; Krayniak & Siegel, 1978a, 1987b; Shanahan et al., 2013; Szekely & Krebs, 1996). Because the focus of this study was to examine the differences in anterior–posterior trajectories we analyzed the above mentioned main neural pathways/long-range connections and mostly skipped the

local circuitry. To do so, we combined our observations with results of former tracing studies and included whether a connection was afferent or efferent or reciprocal (for details see Atoji and Wild, 2004; Shanahan et al., 2013 for review).

Beginning very close to the zero point of the medial level, the interhemispheric fissure (medial telencephalic wall), we observed a massive amount of fibers connecting the hippocampus with the septal region in the dorso-ventral axis that were topographically organized along the anterior–posterior axis (Fig. 7A–D). At this level, direct hypothalamic connections of the PVM and the caudal DMd region of the hippocampus were visible and hippocampal–septal projections to SL and SM were prominent (Fig. 7A–C). More dorsally fibers of the septal region joined the tractus cortico-habenularis et cortico-septalis (CHCS). Fibers that popped out from the dorso-rostral HF to the most medial portion of the tractus septopallio-mesencephalicus (TSM) were also present at this level. The commissural fibers leaving the CPa, curved to the hippocampal–septal junction, ran upwards to the medial wall before they spread into the subdivisions of the HF (caudal route). Most of them originate in the V-complex and DM of the contralateral HF. Visualization of CPa in frontal sections around A 7.50 confirmed this and showed fibers of the V-complex and DM running downwards to the contralateral side, crossing between the two hemispheres indicated by the color-switch, as soon as they reach the contralateral side along the rostral route (Fig. 7D). In the dorsal regions of the HF many thin fibers travel along the anterior–posterior axis connecting anterior and posterior regions (Fig. 7B and D).

Moving more laterally four major pathways were recognized where efferents and afferents pass through the medial wall (Fig. 8A–E). The details of the different paths are presented in Fig. 8B–E. At the lateral level around Lat .50, all subdivisions of the HF along the anterior–posterior axis could be differentiated by the fiber architecture (Fig. 8B) and an additional superficial pathway was recognized at the caudal pole of the HF along Vm and DM where fibers inclines to a 90° direction, i.e., travel in a medial–lateral direction or vice versa (Figs. 7B and 8C). Inspection of the most lateral sagittal slides showed that fibers from caudal CPi, PoA and

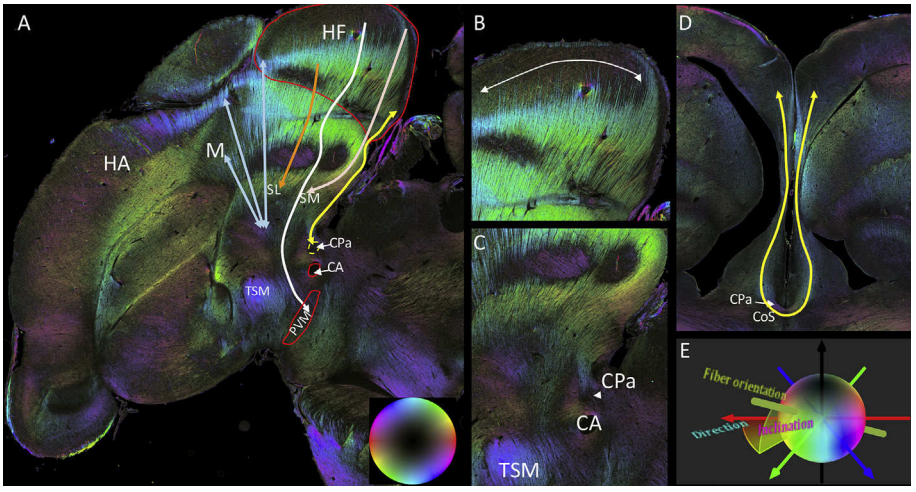

Fig. 7 – The spatial course of massive long-range connections of the hippocampal formation along the anterior–posterior axis. A: 3D-PLI image at the sagittal level around Lat .00 close to the interhemispheric fissure/medial wall. The hue of the color wheel indicates the direction of the in-plane fiber orientation (for explanation see 2.2.2), and the brightness/darkness of the color (e.g., more peripheral/central in the color wheel) indicates a primarily in-plane/through-plane orientation. Red outlines mark the hippocampal formation. White lines show direct connections of the hypothalamus, the nucleus periventricularis magnocellularis (PVM) and the caudal dorsomedial region. Hippocampal–septal connections are indicated by orange lines (lateral septum, SL) and light pink lines (medial septum, SM). The course of commissural fibers running in the commissura pallii (CPa) is marked with yellow. Fibers popping out from the most medial position of the anterior tractus septopallio-mesencephalicus (TSM) are in light blue revealing connections to rostral HF, the hyperpallium apicale (HA) and the mesopallium (M). More dorsally fibers of the septal region belong to the tractus cortico-habenularis et cortico-septalis (CHCS). B: Along the anterior–posterior axis, the V-region and the ventral dorsomedial region (DMv) show a high density of thick fibers or fiber bundles traveling in the dorso-ventral axis that are topographically organized along the anterior–posterior axis, while in the dorsal regions many thin fibers traveling along the anterior–posterior axis connecting anterior and posterior regions (white line). C: Enlargement of the connection between PVM and the dorsomedial region (DM), as well as fiber organization of the CPa and septal regions. D: Visualization of the CPa in a frontal section at A.7.50. As indicated by the color-switch (white arrow), fibers of the V-region and DM cross between the two hemispheres and run upwards to the contralateral side (yellow line). Comparisons between frontal and sagittal sections as well as inclination images show that these fibers stay in plane, i.e., running towards the same level at the anterior–posterior axis they originated. E: Additional legend showing the sinusoidal dependence of the 3D-PLI images. Hemisphere fiber orientations are reflected by hue, saturation and brightness. A change in color corresponds to a change in direction of the fiber. With increased inclination fibers appear in black.

AV as well as intra-hippocampal fibers (reciprocal) connect along this route, while at more medial sagittal levels fibers from SPC join this pathway. The four major pathways included fibers in frontal as well as sagittal sections that connect BSTL and NDB with the HF traveling together from the basal tip of the ventricle along the medial side of the ventricle close to latero-dorsal SL. Further, a few olfactory fibers also join this pathway. Fibers and fiber bundles of the hippocampal connection between SL and SM were additionally separated into two pathways at the level of the nuclei in the septal region (Fig. 8D). The fourth path comprised the crossing fibers of the HF through CPa that get intermingled with the other pathways by passing through the medial wall and then curve separately slightly rostro-ventrally to reach the commissure or vice versa (Fig. 8E).

The visualization of the fiber courses in the tractus CHCS and in the dorsal regions of the HF showed in frontal sections around atlas level A6.50 fibers traveling along the tractus CHCS started to run outwards of DM and the V-region from dorsal to ventral joining the CHCS with increased inclination in caudal direction (Fig. 9A, named post-commissural in Krayniak & Siegel, 1978b). At frontal sections around level A 7.25, at the most caudal point of the septal nuclei SL and SM, some fibers from DL and DM still travel to the medial wall along the periphery of the HF or along the ventricle in a dorso-ventral direction with increased inclination, while a few fibers already started to run further ventrally to SL (Fig. 9B). At both frontal levels, the fiber orientation maps of the DMd and DLd region mostly appeared in dark color, indicating intense fiber intermingling and/or fibers coursing in the anterior–posterior axis (Fig. 9A and B). As verified in the sagittal sections (Fig. 9C), indeed many fibers travel through/from DLd and DMd along the anterior–posterior axis. Those fibers mainly represent the connections between the CPi, the hyperpallium and the HF, as well as intrinsic connections of DM and DL. Fibers from CPi travel dorsally from anterior to posterior along the outer surface of HA reaching the HF at the border of DL (asterisk). In addition, radial fibers from HD, HL and HA cross this fiber tract (arrows), join along its path, and get indistinguishable from olfactory fibers (Fig. 9D). At lateral level Lat 1.00, the CHCS parallels the stria medullaris (SMe) as shown in a sagittal section of the right hemisphere and was clearly separated from the SMe (Fig. 9E). At this level fibers from the habenula, as well as fibers from nucleus taeniae of the amygdala (TnA) have joined the tract.

Around sagittal level Lat 1.80, the fiber courses of TnA that emerged at the ventro(basal)-medial site of the ventricle add to the medial route of afferents from TnA to HF (Fig. 10A). After reaching this point, fibers travel to the caudal end of the hippocampus and then turn into a dorso-medial direction providing the input to the caudal half of the HF. This was verified by inspection of frontal sections around atlas level A 6.25. Fibers travel from TnA medially along the bottom of the ventricle and incline to the caudal pole. Further, we observed that the fiber bundle of TnA and the fiber bundle from the habenula joined the hippocampal–septal bundle at this coordinate (Fig. 10B).

Moving more laterally to level Lat 3.50 the area corticoidea dorsolateralis (CDL) was visible (Fig. 10C and D). The analysis of the connectivity between the HF and the CDL revealed many connections between CDL and DMv, CDL and the V-

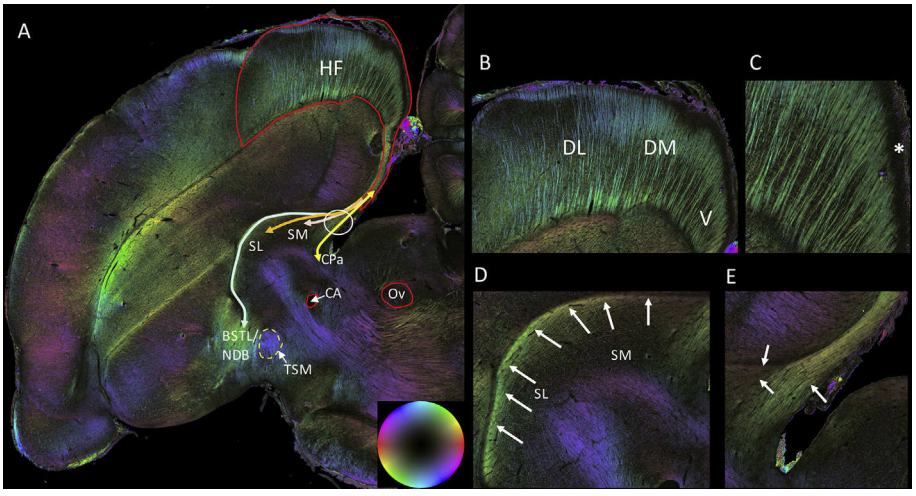

Fig. 8 – Connections of the hippocampal formation in the anterior–posterior axis at the sagittal level around Lat .50. A: Four major branches are recognized at this level were efferents and afferents pass through the medial wall (white circle). The light blue line indicates fibers between the HF and BSTL and NDB that run along this path. B: Zoom into the hippocampal formation (HF) show the organization of fibers running from the medial wall across the V-region, DM and DL. The fiber architecture revealed the subdivisions of the hippocampal formation. C: Zoom into the V-region indicates a superficial pathway at the caudal pole of the hippocampal formation along Vm (white asterisk). D: Zoom into the septal region showing the course of fibers around this region. The white arrows show the pathway of fibers from the HF to NDB and BSTL. E: Zoom into the region were fibers from the septal region and CPa get intermingled indicated by white arrows. CA, commissura anterior; Cpa, commissura pallii; BSTL, lateral part of the bed nucleus of the stria terminalis; NDB, nucleus of the diagonal band; Ov, nucleus ovoidalis; SM, medial septum; SL, lateral septum; TSM, tratcus septopallio-mesencephalicus.

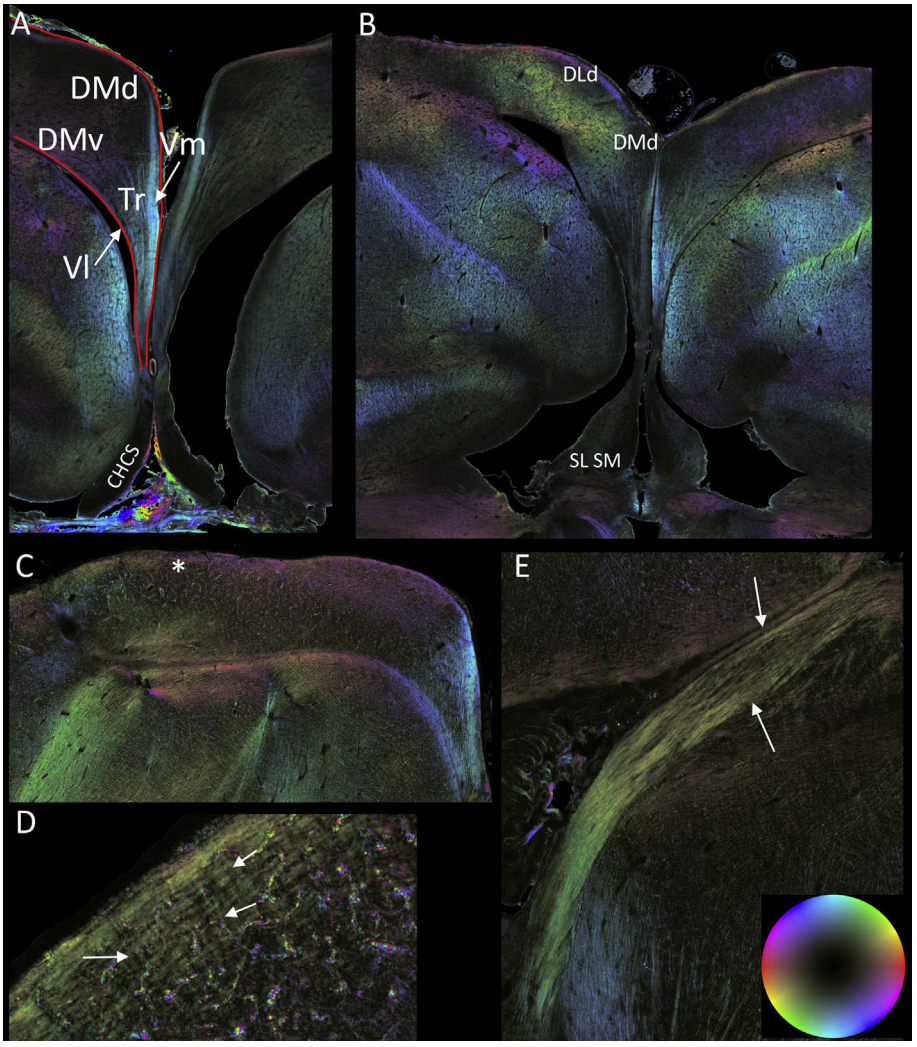

Fig. 9 – Visualization of the fiber courses in the tractus cortico-habenularis et cortico-septalis and in the dorsal regions. A: Detailed 3D-PLI image of the hippocampal formation in a frontal section at atlas level A6.50 showing the tractus cortico-Habenularis et cortico-septalis (CHCS). Fibers begin to run outwards of DM and the V-region running from dorsal to ventral joining the CHCS with increased inclination. B: Frontal section around atlas level A 7.25 at the most caudal point of the septal nuclei SL and SM. Fibers from DL and DM travel dorso-medially along the periphery of the HF or along the ventricle to a ventral direction with increased inclination. In both, (A) and (B), further inspection of the sagittal slices showed that fibers run to the septal nuclei and then travel rostral. Additionally, most of the DMd and DLd region appears dark, indicating intense fiber intermingling and/or fibers coursing in the anterior–posterior axis. As verified in (C) in an example of a sagittal section, indeed many fibers travel through/from DLd and DMd along the anterior–posterior axis. C: Fibers in DMd running in the anterior–posterior axis. Fibers from the cortex piriformis (CPi) travel dorsally from anterior to posterior along the outer surface of HA reaching the hippocampal formation at the border of DL (asterisk). In addition, radial fibers from HA/HL cross this fiber tract (arrows), join along its way particularly from more anterior portions and get indistinguishable from olfactory fibers (D). E: The CHCS parallels the stria medullaris (SMe) in a sagittal section of the right hemisphere around atlas level Lat 1.00 and is clearly separated (see white arrows; CHCS: upper arrow, SMe lower arrow).

region and to a lesser extent between CDL and DMd, and CDL and DL.

3.2. *Adult neurogenesis in the pigeon hippocampal formation along the rostro-caudal axis*

DCX+ cells were differentially expressed in the HF [$\chi^2(n = 9, df = 6) = 51.05$, $p < .001$; Fig. 11A]. The highest numbers were detected in Vl (to all subdivisions of the HF, $p < .01$, except compared to Dlv, $p < .05$) and the lowest in DMd (to all, $p < .01$). Additionally, Tr and Vm showed relatively low levels of DCX expressing cells (to all, $p < .01$, except Tr compared to Vm, $p < .05$). In DLd, DLv and DMv ovoid cells were higher expressed compared to Tr cells (to all $p < .05$), while in Vl more often Tr cells expressed DCX ($p < .01$; Fig. 11A). Along the anterior–posterior axis overall DCX+ cells showed a different distribution in the HF [$\chi^2(n = 9, df = 4) = 17.78$, $p < .01$; Fig. 11B]. The number of DCX+ cells specifically dropped at the most

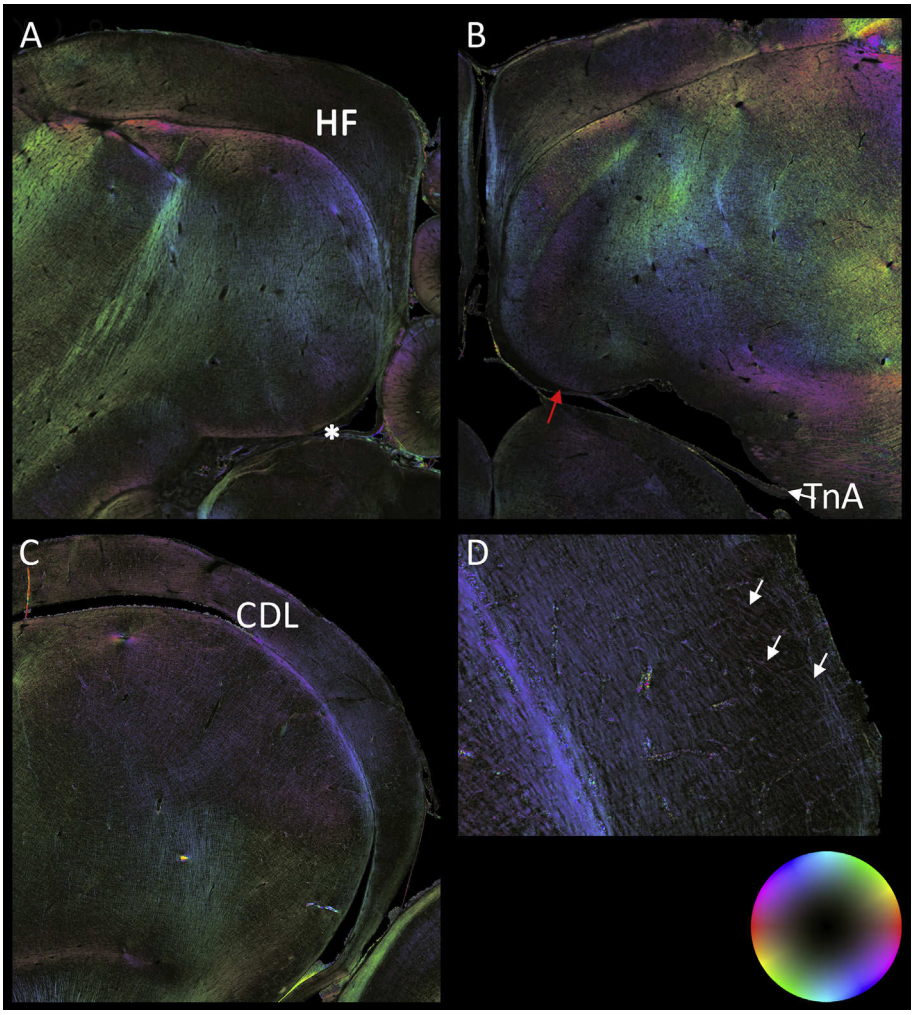

Fig. 10 – Fiber courses of the nucleus taeniae of the amygdala and the area corticoidea dorsolateralis. A: In the sagittal section, the small band of fibers (asterisk) that emerges at the ventro-medial site of the ventricle belongs to the medial route of afferents to the hippocampal formation of TnA. After reaching this point, fibers travel to the caudal end of the hippocampus and then turn into a dorso-medial direction. B: A frontal section that shows the fiber bundle of TnA that provides input to the caudal half of the hippocampus at atlas level A 6.25. As indicated, fibers travel from TnA (white arrow) medially along the bottom of the ventricle and incline (red arrow) to the caudal pole (as shown in A). C: Detail of the fiber architecture of the area corticoidea dorsolateralis (CDL) at a sagittal plane approximately at atlas level Lat 3.50 showing the connectivity of CDL and DM. D: Zoom in to visualize fibers traveling diagonally over DM at more posterior positions (white arrows).

posterior parts of the HF around atlas level A 4.25 ± .5 (to all other atlas levels, $p < .01$). This effect mainly results from a decrease of Tr DCX+ cells at the most posterior level [$\chi^2(n = 9, df = 4) = 12.18$, $p < .05$], while ovoid DCX+ cells were almost equally distributed along the anterior–posterior axis (Fig. 11B). Additionally, very few DCX+/BrdU+ positive cells in the HF were detected, indicating that even after three month of injections of BrdU immature neurons in the pigeon HF are still in a "waiting phase" on their way to mature neurons.

BrdU labeled cells were variably expressed in the subdivisions of the HF [$\chi^2(n = 9, df = 6) = 20.00$, $p < .01$; Fig. 12A], as well as double labeled BrdU+/GFAP+ cells [$\chi^2(n = 9, df = 6) = 26.81$, $p < .001$; Fig. 12A] and BrdU+/NeuN+ cells [$\chi^2(n = 9, df = 6) = 23.12$, $p < .001$; Fig. 12A]. New glial cells [BrdU+/GFAP+] were frequently higher in Vm compared to the other subdivisions (Vm: DLd, $p < .5$, DLv, DMv, Tr, $p < .01$) but not to Vl and DMd (both n.s.). Additionally, lower amounts were detected in Tr compared to DMd and DLv (both $p < .05$). The highest numbers of newborn neurons (BrdU+/NeuN+) were detected in Vl (compared to DLd, DMv, Tr, $p < .05$ and compared to DMd, Vm $p < .01$) and DLv (compared to Tr, DLd, DMd, $p < .05$ and to DMv, Vm, $p < .01$). Only low amounts were found in DMd (compared to Vl, $p < .01$ and to DLd, DLv, DMv, $p < .05$). In all hippocampal subdivisions, the number of newborn glial cells exceeded newborn neurons (all, $p < .01$; Fig. 12A). Along the rostro-caudal axis, no overall differences in BrdU+ [$\chi^2(n = 9, df = 4) = 2.22$, $p = .70$], BrdU+/GFAP+ [$\chi^2(n = 9, df = 4) = 9.16$, $p = .06$] or BrdU+/NeuN+ [$\chi^2(n = 9,$

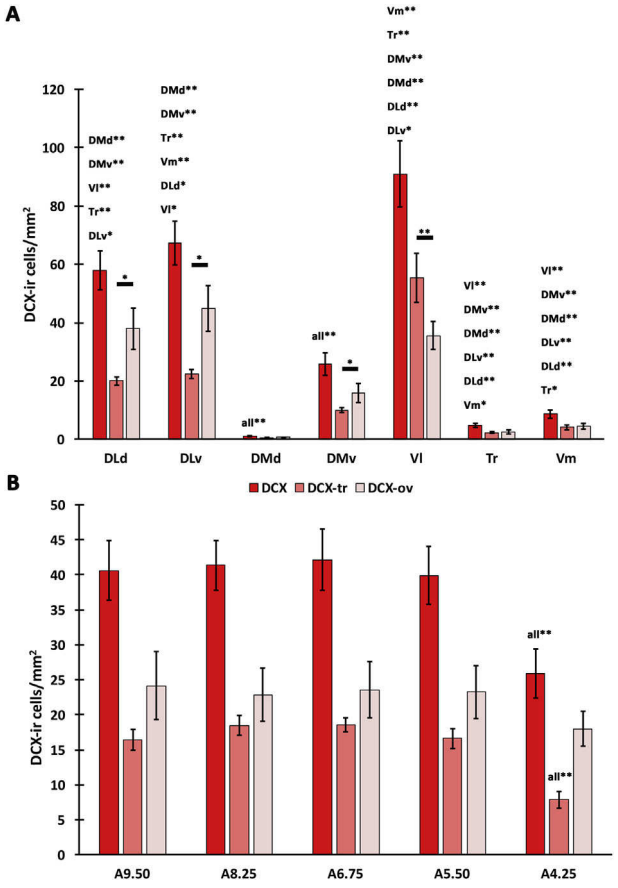

Fig. 11 – Neural plasticity in the adult hippocampal formation of the pigeon. A: Distribution of DCX-ir cells in different subregions of the hippocampal formation (n = 9). B: DCX-ir cells in the hippocampal formation along the anterior–posterior axis. Further, two different types of DCX-ir cells were recognized, triangular (tr-) and ovoid (ov-) cells (n = 9). Bars represent standard error means. Asterisks indicate significant differences (*$p < .05$; **$p < .01$).

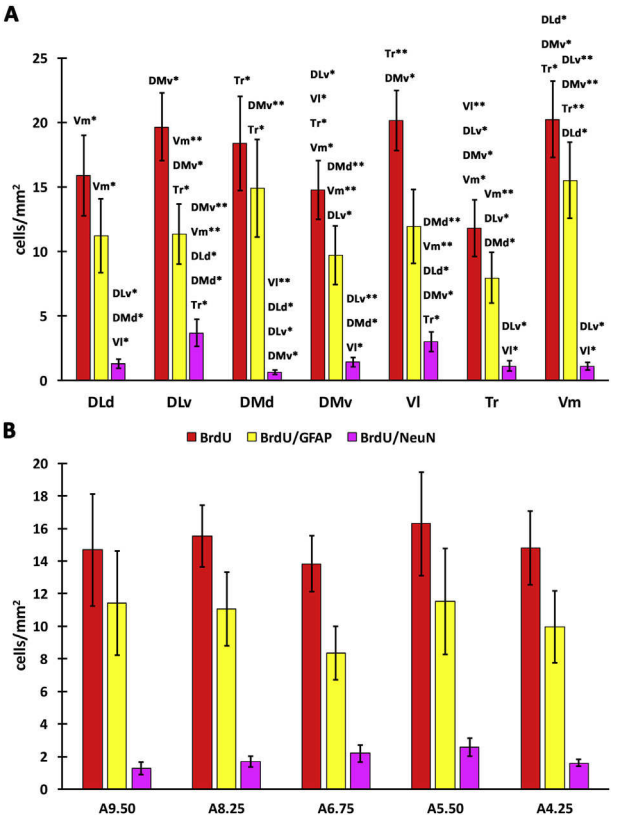

Fig. 12 – Neuro- and gliogenesis in the adult hippocampal formation of the pigeon. A: Distribution of BrdU-ir, BrdU/GFAP-ir, BrdU/NeuN-ir cells in different subregions of the hippocampal formation (n = 9). B: BrdU-ir, BrdU/GFAP-ir, BrdU/NeuN-ir in the hippocampal formation along the anterior–posterior axis (n = 9). Bars represent standard error means. Asterisks indicate significant differences (*$p < .05$; **$p < .01$).

df = 4) = 7.2, $p = .13$] cells in the HF were detected (all Fig. 12B). Selective testing of regions with high or moderate levels of plasticity, respectively Vl, Vm, DLv and DMv (Fig. 13), showed that only in Vl the BrdU+/GFAP+ cells decreased from anterior level 8.25 to posterior level 4.25 [χ^2(n = 9, df = 3) = 9.93, $p < .05$; Fig. 13A].

4. Discussion

The present study disclosed the axonal architecture of the pigeon along the anterior–posterior axis including long range connection using 3D-PLI as a high-resolution imaging approach to study the connectivity structure in the whole brain (Axer, Amunts, et al., 2011; Axer, Gräßel et al., 2011; Schubert et al., 2016; Zilles et al., 2016). It verified that subdivisions of the pigeon HF are partly topographically connected along the anterior–posterior axis with regard to the long-range connectivity and replicated earlier studies of the connectome of the HF in pigeons (Atoji & Wild, 2005; Atoji et al., 2002, 2006; Atoji and Wild, 2004, Casini et al., 1986; Krayniak & Siegel, 1978a, 1987b). To visualize the long-range connections, we used 3D-PLI in two different cutting directions, i.e., sagittal and frontal. The data presented here show for the first time the useful application of 3D-PLI in a bird brain. We furthermore demonstrate regional differences in adult neurogenesis/gliogenesis in individual subdivisions of the pigeon HF (as defined by Herold et al., 2014) by quantitative measures of different markers that have been demonstrated to reliably map neurogenesis in a wide range of species. Here, detailed analysis of five different atlas levels along the anterior–posterior axis indicated higher rates of immature neurons along the axis compared to the most caudal pole of the HF, while globally, matured newborn neurons/glia only showed a trend towards different levels. However, analysis of subdivisions with high or moderate neurogenesis levels showed that newborn glial cells decreased from anterior to posterior levels in the lateral blade of the V-region (Vl). Our

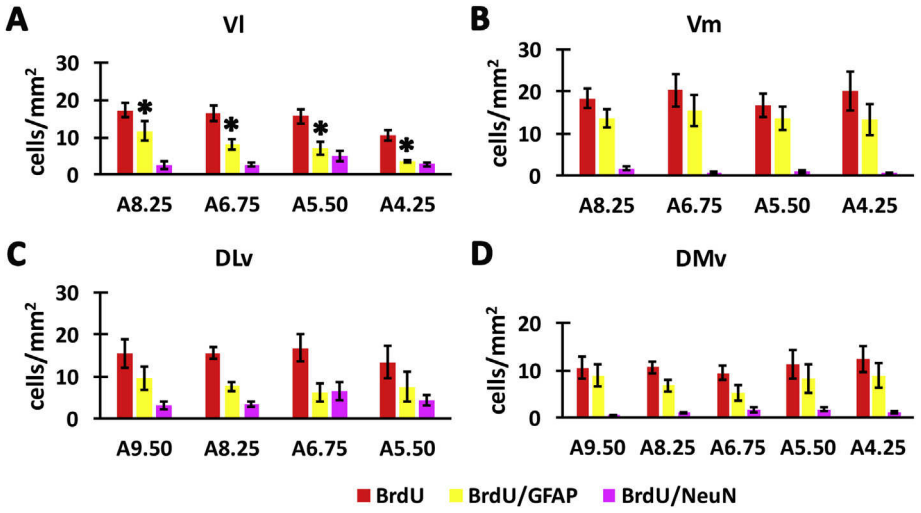

Fig. 13 – Regional distribution of BrdU labeled cells in subdivisions of the hippocampal formation with high or moderate plasticity along the anterior–posterior axis. Only BrdU/GFAP-ir cells in Vl showed decreasing quantities from anterior to posterior coordinates. Bars represent standard error means. Asterisk indicate significant differences (*$p < .05$).

data supports the idea that there is indeed a specialization to regional subdivisions of the HF along the rostro-medial to the caudo-lateral axis of the HF in birds (Smulders, 2017).

4.1. *Connectivity of the hippocampal formation along the anterior–posterior axis in the avian brain*

Numerous studies have investigated the connectome of the avian HF (see Atoji and Wild, 2006; Shanahan et al., 2013; Szekely, 1999 for review), but, none of them did explicitly studied the anterior–posterior axis, although some functional differences were reported in divers bird species. Nevertheless, a few studies mentioned or showed to some extent data of connections along the anterior–posterior axis of the HF (Atoji & Wild, 2004; Atoji et al., 2002; Krayniak & Siegel, 1978a, 1978b; Montagnese, Zachar, Bálint, & Csillag, 2008). In general, the HF projects massively to the septal nuclei and these projections are topographically organized (our data and Atoji & Wild, 2004; Atoji et al., 2002; Krayniak & Siegel, 1978a, 1978b; Montagnese et al., 2008). Caudal HF projects to the post-commissural septum and more rostral HF projects to the rostral septum and the NDB. However, the rostral reciprocal connections to NDB may be more widespread along the anterior–posterior axis according to Atoji and Wild (2002), but are in line with observations from Krayniak and Siegel (1978a). At least, more rostro-medial NDB connects along the medial wall with the HF, while connections with more caudo-lateral NDB were observed with fibers that travel from/to the tip of the ventricle on the same route that connect the HF and the BSTL. According to Atoji et al. (2006), projections from HF to BSTL originate all along the rostro-caudal axis. However, we could not confirm a lateral route from DM to BSTL via the CDL. The inter-hippocampal commissural projections are also topographically organized, i.e., rostral, middle and caudal HF projects to corresponding levels of the contralateral HF. Commissural fibers were organized in a caudal (levels posterior to A 7.5) and a rostral route (levels anterior to A 7.5). These findings are in line with observations by Atoji et al. (2002) and Krayniak and Siegel (1978a). Input from the nucleus taenia (TnA) that belongs to a group of nuclei in the arcopallium/amygdala complex (Herold, Paulitschek, Palomero-Gallagher, Güntürkün, & Zilles, 2018) is limited to the middle/caudal HF to approximately level A 6.25. Fibers between the nucleus posterioris amygdalopallii (PoA) and caudal hippocampal subdivisions course mostly transversally (dorso-laterally) along the outer surface of the telencephalon, while fibers between the ventral arcopallium (AV) or intermediate arcopallium (AI) and the HF use both, the "outer" dorsolateral and the "inner" Vm path along the ventral–medial edge of the ventricle. Hereby, more rostral levels, i.e., more laterally AV fibers travel through the dorsolateral pathway and at more caudal levels, i.e., more medially AV/AIv fibers join the Vm pathway. Whether these two pathways reflect afferent and efferent pathways, or different subtle pathways or only different rostro-caudal connectivity have to be further explored, as well as reinterpretation of data according to the different arcopallial subdivisions (Herold et al., 2018) that receive projections from the HF or vice versa. Both pathways have been described earlier, but with unclear demarcation of the arcopallium/amygdala complex nuclei (Atoji et al., 2002; Casini et al., 1986; Kröner et al., 1999). We further observed a direct connection to the nucleus PVM that was limited to a small portion in caudal DM. This connection was described earlier (Bons, Bouillé, Baylé, & Assenmacher, 1976; Bouillé & Baylé, 1973) and represents afferents from the dorsomedial HF that modulate corticosterone plasma levels. Fibers that join the TSM were limited to the anterior HF, thereby possibly connecting to brain stem sites (Reiner et al., 2004). Further connections with other extrahippocampal structures like hyperpallial subdivisions, olfactory regions or CDL did not differ in their connectivity along the anterior–posterior axis. However, from the border of HA and DL, an enlarging number of thin fibers travel along anterior–posterior axis along the dorsal regions through/over/in DL and DM to the caudal pole of the HF. Before reaching the caudal pole, some of them turn

into the V-region, and then turn ventro-laterally to Vl. To our knowledge, none of the earlier studies mentioned these numerous fibers traveling in the anterior–posterior axis before. To sum up, our results support the idea of a specialization of subdivisions of the HF along the anterior–posterior axis and may also imply functionally different contributions of dorsal and ventral DM and DL. Thereby our results may stimulate future studies to investigate these differences, for example, in relation to spatial learning and emotional behavior.

4.2. *Adult neurogenesis in the hippocampal formation in the avian brain*

In the avian HF adult neurogenesis has been demonstrated for several bird species, including pigeons, zebra finches, canaries, black-capped chickadees, chickens, sparrows, marsh tits, red warblers, corvids and parrots (Balthazart, Charlier, Barker, Yamamura, & Ball, 2008, 2010; Barkan, Roll, Yom-Tov, Wassenaar, & Barnea, 2016; Barnea, Mishal, & Nottebohm, 2006; Hall, Delaney, & Sherry, 2014; Hoshooley, Phillmore, Sherry, & Macdougall-Shackleton, 2007; Kim, Peregrine, & Arnold, 2006; Mazengenya, Bhagwandin, Manger, & Ihunwo, 2018, 2017; Melleu, Pinheiro, Lino-de-Oliveira, & Marino-Neto, 2016, 2013; Meskenaite, Krackow, & Lipp, 2016; Patel, Clayton, & Krebs, 1997; Robertson et al., 2017; Taufique, Prabhat, & Kumar, 2018; Wada, Newman, Hall, Soma, & MacDougall-Shackleton, 2014). However, only few of them have investigated adult neurogenesis in different subdivisions of the HF, and an even smaller number investigated the occurrence of adult neurogenesis regarding to anterior and posterior variations.

A number of markers that are expressed at specific stages during neuronal development or that indicate actively dividing cells have been tested in addition to the "gold standard" BrdU, a thymidine analogue that is inserted into the DNA in actively dividing cells after administration. Doublecortin (DCX), for example, is expressed in many advanced precursor or at an early post-mitotic stage of immature neurons and has been widely accepted as an indicator for adult neurogenesis and neuronal plasticity although some challenges still exist (Balthazart & Ball, 2014; Kremer et al., 2013). Other markers, like Ki67 or PCNA are strictly associated with cell proliferation (Moldovan, Pfander, & Jentsch, 2007; Scholzen & Gerdes, 2000) and Hu expression marks neuronal progenitor cells at an early stage (Barami, Iversen, Furneaux, & Goldman, 1995). NeuN and GFAP on the other hand serve as markers for mature neurons and glia cells. Although most of the antibodies used in this study were used in different species before, including different bird species, we validated the antibodies not only with negative controls but also with Western blot procedures by using fresh brain tissue, and confirmed the correct binding site through protein weights. Immature neurons were verified with DCX, and newborn neurons were proved with BrdU/NeuN double labeling, while newborn glial cells were determined with BrdU/GFAP double labeling.

In pigeons, qualitative and quantitative analysis showed lower amounts of DCX+ cells in Tr and Vm compared to Vl, while DM and DL were only sparsely labeled (Melleu et al., 2013) and lower amounts of DCX+/PCNA+ cells in Vm compared to moderate levels in Tr and Vl, and higher amounts in DL compared to DM (Mazengenya, Bhagwandin, Nkomozepi, Manger, & Ihunwo, 2017). Our quantitative approach confirmed the highest number of DCX+ cells in Vl followed by DLv and DLd, while the lowest numbers of cells/mm^2 were detected in DMd. Further, ovoid migrating immature neurons were more abundant in regions of high to moderate levels of DCX expressing cells, except in Vl, where Tr immature neurons that have already reached their destination were more frequent. We underpinned the DCX results by the finding that mature, adult-born neurons also showed the highest amounts in Vl and DLv, which was determined with BrdU+/NeuN+ labeling after three month of BrdU injections. Functionally, newborn cells in the avian HF have been related to age (Meskenaite et al., 2016), food-deprivation i.e., stress (Robertson et al., 2017; Smulders, 2017), housing, i.e., environmental enrichment (Melleu et al., 2016), food storing (Sherry & Hoshooley, 2010), seasonal changes (Sherry & MacDougall-Shackleton, 2015) and spatial memory (Hall et al., 2014). To our knowledge, none of the studies mentioned earlier in this section studied the genesis of glial cells in the HF. Here we found higher numbers of BrdU+/GFAP+ labeled cells in all estimated subdivisions compared to newborn neurons. In contrast to newborn neurons, newborn glial cells were higher in Vm and DMd compared to all other subdivisions. In general, GFAP+ cells of different size were recognized all over the pigeon HF, with some of them showing long radial branches from the outer surface of Vm and Vl into the Tr region.

Anterior–posterior differences in adult neurogenesis were reported in a study that used radioactive labeled thymidine to mark newborn cells in the HF of black-capped chickadees (Barnea & Nottebohm, 1994). In the study by Barnea and Nottebohm (1994), higher levels of adult neurogenesis in the anterior HF, compared to middle and posterior HF in wild, but not in captive hold birds was demonstrated, which was interpreted in relation to spatial memory acquisition in wild birds visiting different places to collect food. Further, newborn cell numbers were found to decline from anterior to middle to caudal levels, and in relation to the survival time of birds after the injections. In addition, higher levels in the caudal HF of birds that socially interact compared to single caged birds were described (Barnea et al., 2006). The levels of adult neurogenesis changed during season of these food-hoarding species, showing that seasonal changes of behavior affect this rostrocaudal gradient and can result in similar levels of adult neurogenesis in the HF along the anterior–posterior axis (Hoshooley et al., 2007). Under stress conditions, Robertson et al. (2017) reported increased levels of corticosterone plasma levels and reduced levels of newborn cells in the neuronal lineage (BrdU+/Hu+) in food-restricted chicken in rostral HF. However, levels of BrdU+ cells alone decreased in both, caudal and rostral HF after one week of the injection with BrdU. No general differences in BrdU+/Hu+ or BrdU+ cells between rostral and caudal HF were reported, but BrdU+ cells in the ventricular zone showed higher amounts at rostral levels (Robertson et al., 2017). In line with this we found BrdU+/GFAP+ cells gradually decrease from anterior to posterior positions in Vl, showing that a higher number of dividing cells in the more anterior subdivision most likely find their fate in providing an optimal environment for neuronal function and survival. Taken together, our results fit in with former studies, reporting lower amounts of immature neurons at the caudal

pole, and no gradient in overall BrdU+ cells, although none of the studies investigated values for individual subdivisions. In other species, like zebra finches, brown-headed cowbirds and red-winged blackbirds variable neurogenesis levels along the anterior–posterior axis dependent on different housing conditions (social interaction), food storing behavior (spatial memory) and breeding conditions were reported (Barkan et al., 2016; Barnea et al., 2006; Barnea & Nottebohm, 1994; Guigueno, MacDougall-Shackleton, & Sherry, 2016). In our view, more precise studies with respect to the different subdivisions of the HF have to be conducted to relate our findings to functional specializations along the anterior–posterior axis that depend on or impact neurogenesis. Here, our findings provide a foundation upon which future studies can be conducted. Based on previous information on connectivity, neurogenesis, volume change and neurochemical data, Smulders (2017) introduced the idea of a functional specialization of the avian HF along the anterior–posterior axis, and compared the avian anterior pole of the HF to the dorsal pole in rodents (i.e., posterior HF in humans), and the avian posterior pole to the ventral pole in rodents (i.e., anterior HF in humans). Therefore, in the following sections we will now complement this idea with our results by comparing our findings to those in mammals.

4.3. *Comparison to the mammalian hippocampal formation – connectivity*

To date, there is no general consent which subdivisions of the avian HF correspond to their mammalian counterparts, i.e., the DG, CA fields, subiculum and entorhinal cortex, although many similarities between birds and mammals exist at all levels, i.e., anatomical, neurochemical, electrophysiological and functional, many similarities between birds and mammals exist (Abellan et al., 2014; Atoji et al., 2016; Bingman et al., 2017; Herold et al., 2014, 2015; Medina et al., 2017). Some authors argued therefore that thinking about the avian HF in terms of the strict organization such as seen in the mammalian hippocampus is likely insufficient to understand the HF of birds (Bingman & Muzio, 2017; Bingman et al., 2017; Herold et al., 2014, 2015). At the time, most researchers agree that the V-region/DM corresponds to DG/CA-fields and DL corresponds to the entorhinal cortex. Given the remarkable cognitive abilities of birds and the conserved role of the hippocampus in spatial memory, this however, makes the hippocampus of birds an exciting structure to explore the relationship between structure and function against the background of divergent evolutionary paths between mammals and birds of more than 300 Million years. Beside the morphological differences of avian and mammalian hippocampal structures, both structure share many similarities in connectivity (our data; Atoji & Wild, 2006). But what about rostro-caudal differences in connectivity? Strong evidence for a functional specialization along the dorsal–ventral axis (anterior–posterior in primates) of the hippocampus in mammals originate from lesion or inactivation studies (Anacker & Hen, 2017; Colombo et al., 1998; Fanselow & Dong, 2010; O'Leary and Cryan, 2014; Strange et al., 2014; Thompson et al., 2008; Witter et al., 2017). Consequently, the dorsal (septal) hippocampus, which corresponds to the posterior hippocampus in primates is involved in spatial memory and contextual memory encoding and performs primarily cognitive functions, while the ventral (temporal) hippocampus (anterior in primates), processes emotional (stress) and social behavior. Based on the small literature of functional differences in the avian HF along the anterior–posterior axis, this would fit with the idea that the avian anterior pole of the HF corresponds to the septal pole and the posterior HF to the temporal pole of the mammalian HF (Smulders, 2017). Besides, genetic analysis of several marker genes in mice has shown that the hippocampus exhibits different regional and laminar patterns of molecular domains along the dorso-ventral axis and that it can be further compartmentalized in dorsal, intermediate and ventral regions (Fanselow & Dong, 2010; Thompson et al., 2008) that partially overlap with the classification of these domains originally illustrated by Swanson and Cowan (1977). The molecular differences in hippocampal domains are underpinned by anatomic differences in connectivity, which are more prominent between the dorsal and ventral pole, while the intermediate region exhibits a mixture of connections of both, dorsal and ventral parts that discerns on the one hand but have yet not been fully functionally elucidated.

The dorsal (septal, posterior in primates) hippocampus sends massive projections to the dorsal subiculum, while both hippocampus and dorsal subiculum further project to the retrosplenial and anterior cingulate cortices, which are involved in cognitive processing of visuospatial information and memory. The dorsal subicular complex sends further massive parallel projections through the postcommisural fornix to the mammillary nuclei and anterior thalamic regions that in turn project back to the dorsal hippocampus and retrosplenial cortex. Additionally, dorsal CA1 and CA3 project to the caudal and lesser to the dorsal part of the medial zone of the lateral septal complex, which in turn project to the medial septal complex. The lack of a subdivision that is comparable to the subiculum and a more precise classification of the lateral septum (SL) in birds, makes it hard to compare this to the avian situation, but at least we can say that more anterior SL is connected to the anterior DM and further fibers that travel through the TSM connect to anterior DM and DL. Whether these fibers connect the hippocampus to brain stem nuclei and/or diencephalic nuclei or branch to other septal nuclei was not investigated in this study, but will be of interest for future analysis. Based on prior studies, in birds, HF-septal connectivity is less reciprocal, with a significant higher number of afferents from the HF to the septum that is different compared to mammals (Atoji and Wild, 2004; Casini et al., 1986; Montagnese et al., 2004). SL in birds is further receiving a high quantity of visual inputs from diencephalic nuclei, and has prominent connections with hypothalamic nuclei, as well as dopaminergic, serotonergic, noradrenergic and cholinergic inputs (Atoji and Wild, 2004). In addition, the dorsal subiculum as well as the lateral and medial entorhinal cortex of mammals sent further projections to the rostrolateral nucleus accumbens (NAc) and rostral caudate-putamen, which are in turn connected in the so called functional "caudal behavior control column" underlying expression of exploratory behavior, including locomotion, spatial direction and orientation of movements (Swanson & Kalivas, 2000). Direct fiber connections between rostral hippocampal subfields and the NAc were not observed in this study but

between NAc and anterior SL. This finding is in contrast to the tracing study of Atoji et al. (2002) and Atoji and Wild (2004), reporting rostral projections from DL and DM to the medial striatum. However, it is possible that these small number of projections travel under the massive fiber bundles of TSM along the medial wall at the anterior position around A 10.50 (beginning of NAc) and get indistinguishable in our study. Although, no rostro-caudal differences were seen, connectivity to visual areas in the hyperpallium (HA, HL, HD) and the area CDL were confirmed, which in turn connect to the nidopallium caudolaterale (NCL), the analogue of the prefrontal cortex in the pigeon brain and other nidopallial areas (Güntürkün, 2005). This opens up the possibility for the avian HF to connect to higher order areas like the mammalian HF connects to the prefrontal and cingulate areas. Together, our data supports the idea that the anterior hippocampus in birds is stronger involved in visuo-spatial processing but the specialization is less clear compared to the mammalian situation.

The mammalian ventral CA1 on the other hand, projects to several olfactory areas, and shares, together with the ventral subiculum, a bidirectional connectivity to the amygdala nuclei, preferably those that receive massive olfactory inputs (Anderson, Morris, Amaral, Bliss, & O'Keefe, 2007; Cenquizca and Swanson, 2007; Pitkänen et al., 2000; Roberts et al., 2007; Witter & Amaral, 2004). In the pigeon, we confirmed connectivity at medial to caudal levels along the anterior–posterior axis between the HF and the nucleus taeniae of the amygdala (TnA), which is the only amygdala nucleus that receives direct olfactory input from the olfactory bulb according to Patzke, Manns, and Güntürkün (2011). Connectivity to the posterior nucleus of the amygdala (PoA) did not show any specialization along the anterior–posterior axis. In mammals, ventral CA1/subiculum and the amygdala nuclei also share a bidirectional connectivity with pre- and infralimbic and agranular insular cortices (Roberts et al., 2007; Thierry et al., 2000). It was speculated that the hyperpallium densocellulare (HD) in birds shares similarities with the insular cortex of mammals, despite a completely different connectivity (Medina & Reiner, 2000). However, we observed connections between HD and HF, but like the connectivity with the CPi no anterior–posterior specialization was revealed. In mammals, the ventral CA1 and subiculum are further connected either directly or indirectly to the central and medial amygdala, massively to rostral and ventral parts of the lateral septum and the bed nucleus of the stria terminalis to innervate the periventricular and medial zones of the hypothalamus. Thereby, the ventral hippocampus is integrated in a network controlling neuroendocrine, autonomic and somatic motor activities in motivated behaviors, which explains its involvement in fear or aversive learning tasks or stress related responses. Here, direct connections with BSTL were detected but seem to be widespread, while septal connections are topological to the medial and lateral caudal septum. In contrast to SL, the medial septum (SM) is more specifically connected to individual nuclei of the hypothalamus (Atoji and Wild, 2004). In mammals, additionally the ventral CA1 and subiculum, as well as the medial band of the lateral and medial entorhinal cortex give rise to projections to the caudomedial NAc, which plays an important role in reward processing and feeding behavior (Bagot et al., 2015; Walker, Miles, & Davis, 2009). Nothing comparable was observed in the pigeon brain. However, we detected a direct connection of caudal DM with the nucleus PVM, which is the homologue of a portion of the nucleus paraventricularis of the hypothalamus (PVN) in mammals (Berk, 1987). This connection was described earlier in pigeons as projections from the caudal dorsomedial portion of the HF to the PVM (Bons et al., 1976; Bouillé & Baylé, 1973). In mammals, the PVN receives afferents from the subiculum, primary the ventral subiculum (Silverman, Hoffmann, & Zimmermann, 1981) and CA1 (Pakhomova, 1981), which would fit with the theory that caudal HF is comparable to the temporal pole of the HF in mammals, i.e., ventral HF in rodents, and anterior HF in primates.

In rodents, commissural fibers of the hippocampus are organized topographically along the dorso-ventral axis, which is also true for the pigeon anterior–posterior axis. In monkeys, commissural fibers were detected only in the rostral part of both, the DG and the CA fields, whereas the subicular subdivisions and the entorhinal cortex show many commissural connections and most of them are topographically organized (Anderson et al., 2007), while in humans, commissural fibers seem to be absent (Wilson et al., 1991).

Further, we detected numerous thin fibers traveling along anterior–posterior axis along the dorsal regions DLd and DMd. In rodents and monkeys, longitudinally fibers were mostly found in CA3 and DG to propagate information along the septo-temporal axis. CA3 longitudinal fibers originate from the pyramidal cells of the pyramidal layer of CA3, while in DG cells of the hilar region are the source of these fibers that are called associative fibers and are very important for building associative spatial relations between cues and environment (Anderson et al., 2007). In addition, the subiculum gives rise to a longitudinal associative projection that extends from the level of origin to the subiculum at the temporal pole. Recently, in humans, a large number of longitudinally traveling fibers have been observed with 3D-PLI in the alveus of CA1 that are perforant path fibers in the stratum lacunosum-moleculare that cross the hippocampal fissure en route to the dentate molecular layer as well as between entorhinal fibers and the subiculum (Zeineh et al., 2017). However, at the moment, any comparison to the mammalian situation would be purely speculative and our findings of the local circuitry need to be further evaluated by precise tracing studies controlling for the origin of these fibers, although they do not seem to complement the unmyelinated fibers of mossy cells, which would be rarely seen in 3D-PLI due to the maximal sensitivity of PLI to the birefringent properties of myelin.

To sum up, our data and data from tracing studies clearly support a specialization along the anterior–posterior HF in birds, with anterior HF resembling the septal pole and posterior HF resembling the temporal pole of mammals. Further, the finding of a direct connection to PVM with caudal DM as well as the emergence of longitudinal fibers in DM makes it likely that DM exhibits subicular/CA1/CA3 characteristics that need to be revisited and presumably leads to an additional parceling of DM into more subdivisions instead of two (DMd, DMv).

4.4. *Comparison to the mammalian hippocampal formation – adult neurogenesis*

Although deriving from a different neurogenic niche compared to birds, the mammalian hippocampus of diverse species including humans is capable of adult neurogenesis during lifespan, i.e., generating new neurons from neural stem cells in the subgranular zone (but see Bingman et al., 2017; Gage, 2000; Kempermann, 2012; Kempermann et al., 2018; Ming and Song, 2005 for review). In mammals, the highest levels of newborn neurons marked with BrdU and additional markers were detected in DG, while we detected the highest numbers of newborn neurons in the Vl-region. However, in birds, the occurrence of immature neurons appeared not to be exclusively to the V-region but is also prominent in other subdivisions of the HF, including the proposed homologues of CA subfields, subicular and entorhinal cortex, which are relatively sparse labeled with DCX in mammals, although DCX expression is not completely absent (Kremer et al., 2013). This is a major but known species difference, reflecting generally higher levels of plasticity in the avian brain (as well as in fish, reptiles and amphibians) compared to mammals. The same is also true for DCX+ cells that have been detected outside the HF (Ernst & Frisén, 2015; Melleu et al., 2013). In rodents, it has been shown that DCX+ cells have different electrophysiological firing properties compared to mature neurons. This seems to be independent of their brain localization and presumably indicates particular plasticity that is necessary to adapt to environmental changes and to process specific information (Klempin, Kronenberg, Cheung, Kettenmann, & Kempermann, 2011; Spamanato et al., 2012). To our knowledge, no comparable studies in birds exist and thus our findings and those from others should stimulate future electrophysiological studies in birds. However, assuming that the response properties of immature neurons in the avian HF are comparable to those of mammals, birds may have additional mechanisms and faster cellular responses to adopt to environmental changes because they express higher levels of immature neurons.

Equally to the avian HF, adult neurogenesis in mammals varies according to different tasks that have been used to study the role of newborn neurons in relation to function (activity), physiological and pathological stimuli (Christian, Song, & Ming, 2014; Ming & Song, 2011; Snyder, Radik, Wojtowicz, & Cameron, 2009). In mammals, adult neurogenesis in the DG supports memory pattern separation based on space to contextualize (disambiguate) multiple memories (Clelland et al., 2009; Yassa & Stark, 2011), a function that is also supported by the avian HF (Herold et al., 2015). Further, in mammals, adult neurogenesis is involved in inflammatory pain (Zheng et al., 2017), cognitive flexibility (Anacker & Hen, 2017), stress (Tanti et al., 2013) and anxiety/depression like behaviors (O'Leary and Cryan, 2014). In line with anatomical specializations along the dorso-ventral axis, general differences and functional specializations of mammalian ventral and dorsal domains in the context of adult neurogenesis were observed. Generally, DXC+ cells were found at higher levels in the septal (dorsal) pole of the DG of marmosets and mice compared to the temporal (ventral) pole, while proliferating Ki67 + or Ki67+/PCNA+ cells did not differ (Amrein et al., 2015; Anacker & Hen, 2017). Additionally, DCX+ cells were generally higher in the suprapyramidal blade compared to the infrapyramidal blade and radial glia/progenitor cells were detected at lower levels in the infrapyramidal blade of ventral DG compared to all DG subdivisions (Jinno, 2011). Higher levels of DCX+ cells were also observed in canine dorsal hippocampus (Lowe et al., 2015). In the dorsal hippocampus of rats, DCX+, BrdU+, Ki67+ and BrdU+/DCX+ cells showed higher levels compared to ventral 9 days after BrdU injections (Ho & Wang, 2010). In line with these observations our data complement those findings and show further similarities between the avian and mammalian HF. Interestingly, we also found differences in the number of DCX+ cells and BrdU/NeuN+ newborn neurons between Vl and Vm, with higher levels of adult neurogenesis in Vl compared to Vm. In our study, pigeons generally lived in an enriched environment in their loft and were allowed to fly freely. Further, in rodents that performed complex spatial and contextual stimulation in an enriched environment neurogenesis was increased in dorsal DG (Kempermann, Kuhn, & Gage, 1997; Snyder et al., 2009; Tanti et al., 2012, 2013), while exposure to chronic stress severely reduces levels of proliferation, differentiation and survival of neurons in the ventral DG but also affects dorsal portions to some levels if simultaneously contextual memory learning is acquired (Anacker & Hen, 2017; Hawley, Morch, Christie, & Leasure, 2012; O'Leary and Cryan, 2014; Snyder et al., 2009; Tanti et al., 2013). Together, data from neurogenesis experiments further point to similarities of septal HC in mammals and anterior HF in birds, and temporal HC and posterior HF. However, one recent study in chickens showed that food deprivation, which was accompanied by increased corticosterone levels results in decreased levels of neuronal progenitors in the rostral pole, while new neurons decreased in both, caudal and rostral poles (Robertson et al., 2017). However, in rodents it was shown that sometimes chronic stress also affects neurogenesis in the septal pole, and seems to be highly dependent on the context in which animals were tested (Ho & Wang, 2010; O'Leary and Cryan, 2014; Snyder et al., 2009). Clearly more functional studies in birds, as well as in mammals are needed that explore the relationship of adult neurogenesis and functional specialization along the septo-temporal axis to a better understanding of these interactions.

4.5. *Evolutionary connectomics*

The hippocampus in all vertebrates emerges during development from the same dorsomedial region of the procencephalic alar plate (Bingman, Salas, & Rodriguez, 2009; Butler & Hodos, 2005; Hevner, 2016; Nomura & Hirata, 2017; Striedter, 2005), except ray-finned fish, where the homologue is at a dorsolateral position, which adopts because the embryonic telencephalon does not evaginate but, instead, everts (Striedter & Northcutt, 2006). In non-mammalian species, the homologue of the hippocampus is called medial or dorsomedial pallium (Hevner, 2016). During more than 300 Million years of separate evolution from a basal hippocampus of amphibians or non-sauropsids, compared to both, avian and mammalian

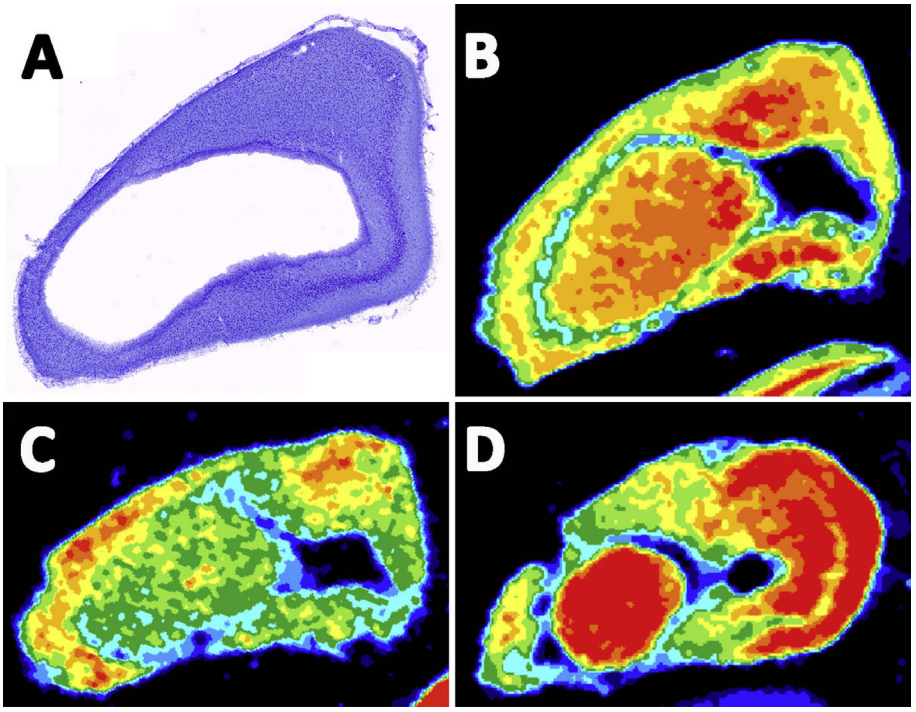

Fig. 14 – The caudal V-region of the pigeon hippocampus. A: Nissl staining showing the tri-laminated part of the V-region in a coronal section at approximately atlas level A 3.50–3.25. B–D: AMPA (B), Kainate (C) and NMDA (D) receptor expression in the caudal V-region (supplementary data figures not shown in Herold et al., 2014). Red indicates high densities while blue indicates low densities. Scales are different.

hippocampi have increased in size and complexity and evolved different cytoarchitectonical organizations (Bingman et al., 2017; Striedter, 2016). Further positional changes occurred. While in reptiles and birds, the HF is largely located periventricular in a dorsal region of the medial wall of the telencephalon, in mammals, only the primordium of the hippocampal complex (fimbria, DG, Ammon's horn, subiculum, and entorhinal cortex) is located dorso-medially but comes to lie ventrally within the development of the neocortices. In addition, the DG becomes variably convoluted among mammals (Hevner, 2016; Witter et al., 2017). However, a thin remnant of the HF surrounds the splenium of the corpus callosum that ascends dorsally over the corpus callosum to form the induseum griseum, which comprises remnants of the subiculum and other fields of the HF (Anderson et al., 2007).

In the hippocampus of reptiles, tri-lamination emerged that was accompanied by an enlargement of other pallial regions, while in birds, the HF displays a more cellular structure reflecting a presumptive reduction of lamination that was accompanied by a substantial increase in hippocampus size (Bingman et al., 2017; Hevner, 2016; Striedter, 2016). In mammals, lamination occurs inside-out in the HF, accept in DG were migration occurs outside-in. This process strongly depends on radial glia scaffold and reelin secretion of Cajal-Retzius cells (Frotscher & Seress, 2007). Cajal-Retzius cells are also prominent during development of the avian medial pallium (Nomura, Takahashi, Hara, & Osumi, 2008) but in contrast to the mammalian medial pallium do not migrate to the dorsal preplate, nor do other progenitor cells from the cortical hem or the medial pallium give rise to migrating cells to the dorsal pallium (García-Moreno et al., 2018). However, this seems to be different from lizards (Cabrera-Soccoro et al., 2007), and needs to be further explored along the axis of the cortical hem/medial pallium, but may be one reason of the different structure of mammalian, reptilian and avian hippocampal as well as neocortical regions. In case of the avian hippocampus, which derives from a more dorsomedial position and has largely expanded, this might also explain the different morphology of the most caudal–ventral parts of the V-region, where a clear tri-laminar structure is visible (Fig. 14) compared to more rostral parts of the V-region, where the cellular line splits up into two blades or becomes convoluted. Analysis of single-cell transcriptomics of the reptilian medial most pallium, particularly the dorsomedial cortex, has been shown that preliminary precursors of the hippocampal regions, including the DG, cornu ammonis 1 (CA1) and cornu ammonis (CA3) were already present in the ancestor of all amniotes (Tosches et al., 2018), which is also supported by a recently developmental analysis of chick, lizard and mouse hippocampus by Medina et al. (2017). These findings and our recent data, however, make it unlikely that the DG has recently evolved as an add-on structure of the mammalian species suggested earlier by Kempermann (2012). Instead an anlage of the DG in the least common ancestor must have been already existed that was highly morphologically transformed during million years of separate evolution with still conserved functionality.

5. Conclusion

Birds have extraordinary cognitive abilities that even exceed those of some primates, and they achieve this even without a layered structure of their pallial derivatives but with conserved functional loops between brain structures, including hippocampal connectivity and some similar properties of cells contributing to these circuits. In addition, in many cases the organization principles of hippocampal network connectivity, i.e., anterior–posterior differences seem to be conserved. On the other hand, over more than 300 Million years of separate evolution in adaption to an ecologic niche may have led to further neuronal specializations resembling an alternative route to functionally adopt, reaching the apex of avian evolution in a highly competitive world among other animals including humans. Moreover, high forms of plasticity in the avian brain, validated by DCX expression in various brain regions, may indicate the promotion of further development and evolution of brain structures, and perhaps the ability for rapid adaptation to environmental changes, which may be a selective advantage at some point.

Funding

The 3D-PLI related part of the presented study was supported by the European Union's Horizon 2020 Research and Innovation Program under Grant Agreement No. 720270 (Human Brain Project, SGA1) and No. 785907 (Human Brain Project, SGA2).

Acknowledgments

We thank Nicole Delhaes for preparing the immunohistochemistry and the Western Blots and Isabelle Masson and Dustin Hullin for help with the cell counting. We would also like to thank Christian Schramm, Patrick Nysten and Steffen Werner for preparing the pigeon brain slices for the 3D-PLI experiments and Karl Zilles for help with the data interpretation in the beginning of the 3D-PLI experiments. The authors gratefully acknowledge the computing time granted through JARA-HPC on the supercomputer JURECA at Forschungszentrum Jülich. We further thank David Gräßel who supervised the 3D-PLI work, helped with the preparation of 3D-PLI data and the methods section.

REFERENCES

Abellan, A., Desfilis, E., & Medina, L. (2014). Combinatorial expression of Lef1, Lhx2, Lhx5, Lhx9, Lmo3, Lmo4, and Prox1 helps to identify comparable subdivisions in the developing hippocampal formation of mouse and chicken. *Frontiers in Neuroanatomy, 4*, 8–59.

Amrein, I., Nosswitz, M., Slomianka, L., van Dijk, R. M., Engler, S., Klaus, F., et al. (2015). Septo-temporal distribution and lineage progression of hippocampal neurogenesis in a primate (Callithrix jacchus) in comparison to mice. *Frontiers in Neuroanatomy, 9*, 85. https://doi.org/10.3389/fnana.2015.00085.

Anacker, C., & Hen, R. (2017). Adult hippocampal neurogenesis and cognitive flexibility – linking memory and mood. *Nature Reviews. Neuroscience, 18*, 335–346.

Anderson, P., Morris, R., Amaral, D., Bliss, T., & O'Keefe, J. (2007). *The hippocampus book*. Oxford University Press.

Atoji, Y., Saito, S., & Wild, J. M. (2006). Fiber connections of the compact division of the posterior pallial amygdala and lateral part of the bed nucleus of the stria terminalis in the pigeon (Columba livia). *Journal of Comparative Neurology, 499*, 161–182.

Atoji, Y., Sarkar, S., & Wild, J. M. (2016). Proposed homology of the dorsomedial subdivision and V-shaped layer of the avian hippocampus to Ammon's horn and dentate gyrus, respectively. *Hippocampus, 26*, 1608–1617.

Atoji, Y., & Wild, J. M. (2004). Fiber connections of the hippocampal formation and septum and subdivisions of the hippocampal formation in the pigeon as revealed by tract-tracing and kainic acid lesions. *Journal of Comparative Neurology, 475*, 426–461.

Atoji, Y., & Wild, J. M. (2005). Afferent and efferent connections of the dorsolateral corticoid area and a comparison with connections of the temporo-parieto-occipital area in the pigeon (Columba livia). *Journal of Comparative Neurology, 485*, 165–182.

Atoji, Y., & Wild, J. M. (2006). Anatomy of the avian hippocampal formation. *Reviews in the Neurosciences, 17*, 3–15.

Atoji, Y., Wild, J. M., Yamamoto, Y., & Suzuki, Y. (2002). Intratelencephalic connections of the hippocampus in pigeons (Columba livia). *Journal of Comparative Neurology, 447*, 177–199.

Axer, M., Amunts, K., Gräßel, D., Palm, C., Dammers, J., Axer, H., et al. (2011). A novel approach to the human connectome: Ultra-high resolution mapping of fiber tracts in the brain. *NeuroImage, 54*, 1091–1101. https://doi.org/10.1016/j.neuroimage.2010.08.075.

Axer, M., Gräßel, D., Kleiner, M., Dammers, J., Dickscheid, T., Reckfort, J., et al. (2011). High-resolution fiber tract reconstruction in the human brain by means of three-dimensional polarized light imaging. *Frontiers in Neuroinformatics, 5*(34). https://doi.org/10.3389/fninf.2011.00034.

Bagot, R. C., Parise, E. M., Peña, C. J., Zhang, H. X., Maze, I., Chaudhury, D., et al. (2015). Ventral hippocampal afferents to the nucleus accumbens regulate susceptibility to depression. *Nature Communications, 6*, 7062. https://doi.org/10.1038/ncomms8062.

Balthazart, J., & Ball, G. (2014). Doublecortin is a highly valuable endogenous marker of adult neurogenesis in canaries. *Brain, Behavior and Evolution, 84*, 1–4.

Balthazart, J., Boseret, G., Konkle, A. T. M., Hurley, L. L., & Ball, G. F. (2008). Doublecortin as a marker of adult neuroplasticity in the canary song control nucleus HVC. *The European Journal of Neuroscience, 27*, 801–817.

Balthazart, J., Charlier, T. D., Barker, J. M., Yamamura, T., & Ball, G. F. (2010). Sex steroid-induced neuroplasticity and behavioural activation in birds. *The European Journal of Neuroscience, 32*, 2116–2132.

Barami, K., Iversen, K., Furneaux, H., & Goldman, S. A. (1995). Hu protein as an early marker of neuronal phenotypic differentiation by subependymal zone cells of the adult songbird forebrain. *Journal of Neurobiology, 28*, 82–101.

Barkan, S., Roll, U., Yom-Tov, Y., Wassenaar, L. I., & Barnea, A. (2016). Possible linkage between neuronal recruitment and flight distance in migratory birds. *Scientific Reports, 6*, 21983. https://doi.org/10.1038/srep21983.

Barnea, A., Mishal, A., & Nottebohm, F. (2006). Social and spatial changes induce multiple survival regimes for new neurons in two regions of the adult brain: An anatomical representation of time? *Behavioural Brain Research, 167*, 63–74.

Barnea, A., & Nottebohm, F. (1994). Seasonal recruitment of hippocampal neurons in adult free-ranging black-capped chickadees. *Proceedings of the National Academy of Sciences of the United States of America, 91*, 11217–11221.

Benowitz, L. I., & Karten, H. J. (1976). The tractus infundibuli and other afferents to the parahippocampal region of the pigeon. *Brain Research, 102*, 174–180.

Berk, M. L. (1987). Projections of the lateral hypothalamus and bed nucleus of the stria terminalis to the dorsal vagal complex in the pigeon. *Journal of Comparative Neurology, 260*, 140–156.

Bingman, V. P., & Muzio, R. N. (2017). Reflections on the structural-functional evolution of the hippocampus: What is the big deal about a dentate gyrus? *Brain, Behavior and Evolution, 90*, 53–61. https://doi.org/10.1159/000479095.

Bingman, V. P., Rodriguez, F., & Salas, C. (2017). The hippocampus of nonmammalian vertebrates. *Evolution of Nervous Systems, 2nd ed., 1*, 479–489. https://doi.org/10.1016/B978-0-12-804042-3.00013-0.

Bingman, V. P., Salas, C., & Rodriguez, F. (2009). Evolution of the hippocampus. In *Encyclopedia of neuroscience* (pp. 1356–1360). Berlin, Heidelberg: Springer.

Bolhuis, J. J., & Wynne, C. D. (2009). Can evolution explain how minds work? *Nature, 458*, 832–833. https://doi.org/10.1038/458832a.

Bons, N., Bouillé, C., Baylé, J. D., & Assenmacher, I. (1976). Light and electron microscopic evidence of hypothalamic afferences originating from the hippocampus in the pigeon. *Experientia, 32*(11), 1443–1445.

Bouillé, C., & Baylé, J. D. (1973). Effects of limbic stimulations or lesions on basal and stress-induced hypothalamic-pituitary-adrenocortical activity in the pigeon. *Neuroendocrinology, 13*, 264–277. https://doi.org/10.1159/000122211.

Butler, A. B., & Hodos, W. (2005). *Comparative vertebrate neuroanatomy: Evolution and adaptation*. John Wiley & Sons.

Butler, A. B., Reiner, A., & Karten, H. J. (2011). Evolution of the amniote pallium and the origins of mammalian neocortex. *Annals of the New York Academy of Sciences, 1225*, 14–27. https://doi.org/10.1111/j. 1749-6632. 2011.06006.x.

Cabrera-Socorro, A., Hernandez-Acosta, N. C., Gonzalez-Gomez, M., & Meyer, G. (2007). Comparative aspects of p73 and Reelin expression in Cajal-Retzius cells and the cortical hem in lizard, mouse and human. *Brain Research, 1132*, 59–70.

Casini, G., Bingman, V. P., & Bagnoli, P. (1986). Connections of the pigeon dorsomedial forebrain studied with WGA-HRP and 3H-proline. *Journal of Comparative Neurology, 245*, 454–470.

Cenquizca, L. A., & Swanson, L. W. (2007). Spatial organization of direct hippocampal field CA1 axonal projections to the rest of the cerebral cortex. *Brain Research Reviews, 56*, 1–26.

Chakraborty, M., & Jarvis, E. D. (2015). Brain evolution by brain pathway duplication. *Philosophical Transactions of the Royal Society of London. Series B, Biological sciences, 370*. https://doi.org/10.1098/rstb.2015.0056. pii: 20150056.

Christian, K. M., Song, H., & Ming, G. L. (2014). Functions and dysfunctions of adult hippocampal neurogenesis. *Annual Review of Neuroscience, 37*, 243–262. https://doi.org/10.1146/annurev-neuro-071013-014134.

Clelland, C. D., Choi, M., Romberg, C., Clemenson, G. D., Jr., Fragniere, A., Tyers, P., et al. (2009). A functional role for adult hippocampal neurogenesis in spatial pattern separation. *Science, 325*, 210–213. https://doi.org/10.1126/science.1173215.

Colombo, M., & Broadbent, N. (2000). Is the avian hippocampus a functional homologue of the mammalian hippocampus? *Neuroscience and Biobehavioral Reviews, 24*, 465–484.

Colombo, M., Fernandez, T., Nakamura, K., & Gross, C. G. (1998). Functional differentiation along the anterior-posterior axis of the hippocampus in monkeys. *Journal of Neurophysiology, 80*, 1002–1005.

Dong, H.-W., Swanson, L. W., Chen, L., Fanselow, M. S., & Toga, A. W. (2009). Genomic–anatomic evidence for distinct functional domains in hippocampal field CA1. *Proceedings of the National Academy of Sciences of the United States of America, 106*, 11794–11799.

Ernst, A., & Frisén, J. (2015). Adult neurogenesis in humans – common and unique traits in mammals. *PLoS Biology, 13*, e1002045. https://doi.org/10.1371/journal.pbio. 1002045.

Fanselow, M. S., & Dong, H. W. (2010). Are the dorsal and ventral hippocampus functionally distinct structures? *Neuron, 65*, 7–19.

Frotscher, M., & Seress, L. (2007). Morphological development of the hippocampus. In *The hippocampus book*. Oxford University Press.

Gabi, M., Neves, K., Masseron, C., Ribeiro, P. F., Ventura-Antunes, L., Torres, L., et al. (2016). No relative expansion of the number of prefrontal neurons in primate and human evolution. *Proceedings of the National Academy of Sciences of the United States of America, 113*, 9617–9622.

Gage, F. H. (2000). Mammalian neural stem cells. *Science, 287*, 1433–1438. https://doi.org/10.1126/science.287.5457.1433.

Gagliardo, A., Ioale, P., & Bingman, V. P. (1999). Homing in pigeons: The role of the hippocampal formation in the representation of landmarks used for navigation. *The Journal of Neuroscience: the Official Journal of the Society for Neuroscience, 19*, 311–315.

García-Moreno, F., Anderton, E., Jankowska, M., Begbie, J., Encinas, J. M., Irimia, M., et al. (2018). Absence of tangentially migrating glutamatergic neurons in the developing avian brain. *Cell Reports, 22*, 96–109. https://doi.org/10.1016/j.celrep.2017.12.032.

Guigueno, M. F., MacDougall-Shackleton, S. A., & Sherry, D. F. (2016). Sex and seasonal differences in hippocampal volume and neurogenesis in brood-parasitic brown-headed cowbirds (Molothrus ater). *Developmental Neurobiology, 76*, 1275–1290.

Güntürkün, O. (2005). The avian 'prefrontal cortex' and cognition. *Current Opinion in Neurobiology, 15*, 686–693.

Güntürkün, O., & Bugnyar, T. (2016). Cognition without cortex. *Trends in Cognitive Sciences, 20*, 291–303. https://doi.org/10.1016/j.tics.2016.02.001.

Güntürkün, O., Ströckens, F., Scarf, D., & Colombo, M. (2017). Apes, feathered apes, and pigeons: Differences and similarities. *Current Opinion in Behavioral Sciences, 16*, 35–40.

Hall, Z. J., Delaney, S., & Sherry, D. F. (2014). Inhibition of cell proliferation in black-capped chickadees suggests a role for neurogenesis in spatial learning. *Developmental Neurobiology, 74*, 1002–1010. https://doi.org/10.1002/dneu.22180.

Hawley, D. F., Morch, K., Christie, B. R., & Leasure, J. L. (2012). Differential response of hippocampal subregions to stress and learning. *PLoS One, 7*, e53126. https://doi.org/10.1371/journal.pone.0053126.

Herculano-Houzel, S., Catania, K., Manger, P. R., & Kaas, J. H. (2015). Mammalian brains are made of these: A dataset of the numbers and densities of neuronal and nonneuronal cells in the brain of glires, primates, scandentia, eulipotyphlans afrotherians and artiodactyls, and their relationship with body mass. *Brain, Behavior and Evolution, 86*, 145–163.

Herold, C., Bingman, V. P., Ströckens, F., Letzner, S., Sauvage, M., Palomero-Gallagher, N., et al. (2014). Distribution of neurotransmitter receptors and zinc in the pigeon (Columba livia) hippocampal formation: A basis for further comparison with the mammalian hippocampus. *Journal of Comparative Neurology, 522*, 2553–2575.

Herold, C., Coppola, V. J., & Bingman, V. P. (2015). The maturation of research into the avian hippocampal formation: Recent discoveries from one of the nature's foremost navigators. *Hippocampus, 25*, 1193–1211.

Herold, C., Paulitschek, C., Palomero-Gallagher, N., Güntürkün, O., & Zilles, K. (2018). Transmitter receptors reveal segregation of the arcopallium/amygdala complex in pigeons (Columba livia). *Journal of Comparative Neurology, 526*, 439–466.

Hevner, R. F. (2016). Evolution of the mammalian dentate gyrus. *Journal of Comparative Neurology, 524*, 578–594.
Hoshooley, J. S., Phillmore, L. S., Sherry, D. F., & Macdougall-Shackleton, S. A. (2007). Annual cycle of the black-capped chickadee: Seasonality of food-storing and the hippocampus. *Brain, Behavior and Evolution, 69*, 161–168.
Hough, G. E., 2nd, Pang, K. C., & Bingman, V. P. (2002). Intrahippocampal connections in the pigeon (Columba livia) as revealed by stimulation evoked field potentials. *Journal of Comparative Neurology, 452*, 297–309.
Ho, Y. C., & Wang, S. (2010). Adult neurogenesis is reduced in the dorsal hippocampus of rats displaying learned helplessness behavior. *Neuroscience, 171*, 153–161.
Jinno, S. (2011). Topographic differences in adult neurogenesis in the mouse hippocampus: A stereology-based study using endogenous markers. *Hippocampus, 21*, 467–480.
Jones, R. C. (1941). A new calculus for the treatment of optical systems. *Journal of the Optical Society of America, 31*, 488–493.
Kaas, J. H., & Stepniewska, I. (2015). Evolution of posterior parietal cortex and parietal-frontal networks for specific actions in primates. *Journal of Comparative Neurology*, 524, 595–608. https://doi.org/10.1002/cne.23838.
Karten, H. J. (2015). Vertebrate brains and evolutionary connectomics: On the origins of the mammalian 'neocortex'. *Philosophical Transactions of the Royal Society of London. Series B, Biological sciences, 370*. https://doi.org/10.1098/rstb.2015.0060. pii: 20150060.
Karten, H. J., & Hodos, W. (1967). *A stereotaxic atlas of the brain of the pigeon (Columba livia)*. Baltimore: John Hopkins University Press.
Kempermann, G. (2012). New neurons for "survival of the fittest. *Nature Reviews. Neuroscience, 13*, 727–736.
Kempermann, G., Gage, F. H., Aigner, L., Song, H., Curtis, M. A., Thuret, S., et al. (2018). Human adult neurogenesis: Evidence and remaining questions. *Cell Stem Cell*. https://doi.org/10.1016/j.stem.2018.04.004. pii: S1934-5909(18)30166-30168.
Kempermann, G., Kuhn, H. G., & Gage, F. H. (1997). More hippocampal neurons in adult mice living in an enriched environment. *Nature, 386*, 493–495.
Kim, Y. H., Peregrine, J., & Arnold, A. P. (2006). The distribution of expression of doublecortin (DCX) mRNA and protein in the zebra finch brain. *Brain Research, 1106*, 189–196.
Klempin, F., Kronenberg, G., Cheung, G., Kettenmann, H., & Kempermann, G. (2011). Properties of doublecortin-(DCX)-expressing cells in the piriform cortex compared to the neurogenic dentate gyrus of adult mice. *PLoS One, 6*, e25760. https://doi.org/10.1371/journal.pone.0025760.
Krayniak, P. F., & Siegel, A. (1978a). Efferent connections of the hippocampus and adjacent regions in the cortex. *Brain, Behavior and Evolution, 15*, 372–388.
Krayniak, P. F., & Siegel, A. (1978b). Efferent connections of the septal area in the pigeon. *Brain, Behavior and Evolution, 15*, 389–404.
Krebs, J. R., Erichsen, J. T., & Bingman, V. P. (1991). The distribution of neurotransmitters and neurotransmitter-related enzymes in the dorsomedial telencephalon of the pigeon (Columba livia). *Journal of Comparative Neurology, 314*, 467–477.
Kremer, T., Jagasia, R., Herrmann, A., Matile, H., Borroni, E., Francis, F., et al. (2013). Analysis of adult neurogenesis: Evidence for a prominent "non-neurogenic" DCX protein pool in rodent brain. *PLoS One, 8*(5). https://doi.org/10.1371/journal.pone.0059269. e59269.
Kröner, S., & Güntürkün, O. (1999). Afferent and efferent connections of the caudolaterale neostriatum in the pigeon (Columba livia): A retro-and anterograde pathway tracing study. *Journal of Comparative Neurology, 407*, 228–260.
Lowe, A., Dalton, M., Sidhu, K., Sachdev, P., Reynolds, B., & Valenzuela, M. (2015). Neurogenesis and precursor cell differences in the dorsal and ventral adult canine hippocampus. *Neuroscience Letters, 593*, 107–113. https://doi.org/10.1016/j.neulet.2015.03.017.
MacPhail, E. M. (2002). The role of the avian hippocampus in spatial memory. *Psicológica, 23*, 93–108.
Mazengenya, P., Bhagwandin, A., Manger, P. R., & Ihunwo, A. O. (2018). Putative adult neurogenesis in old world parrots: The Congo African grey parrot (Psittacus erithacus) and Timneh grey parrot (Psittacus timneh). *Frontiers in Neuroanatomy, 12*, 7. https://doi.org/10.3389/fnana.2018.00007.
Mazengenya, P., Bhagwandin, A., Nkomozepi, P., Manger, P. R., & Ihunwo, A. O. (2017). Putative adult neurogenesis in two domestic pigeon breeds (Columba livia domestica): Racing homer versus utility carneau pigeons. *Neural Regeneration Research, 12*, 1086–1096. https://doi.org/10.4103/1673-5374.211187.
Medina, L., & Abellan, A. (2009). Development and evolution of the pallium. *Seminars in Cell & Developmental Biology, 20*, 698–711.
Medina, L., Abellán, A., & Desfilis, E. (2017). Contribution of genoarchitecture to understanding hippocampal evolution and development. *Brain, Behavior and Evolution, 90*, 25–40. https://doi.org/10.1159/000477558.
Medina, L., & Reiner, A. (2000). Do birds possess homologues of mammalian primary visual, somatosensory and motor cortices? *Trends in Neurosciences, 23*, 1–12.
Melleu, F. F., Pinheiro, M. V., Lino-de-Oliveira, C., & Marino-Neto, J. (2016 May). Defensive behaviors and prosencephalic neurogenesis in pigeons (Columba livia) are affected by environmental enrichment in adulthood. *Brain Structure & Function, 221*(4), 2287–2301. https://doi.org/10.1007/s00429-015-1043-6.
Melleu, F. F., Santos, T. S., Lino-de-Oliveira, C., & Marino-Neto, J. (2013). Distribution and characterization of doublecortin-expressing cells and fibers in the brain of the adult pigeon (Columba livia). *Journal of Chemical Neuroanatomy, 47*, 57–70. https://doi.org/10.1016/j.jchemneu.2012.10.006.
Meskenaite, V., Krackow, S., & Lipp, H. P. (2016). Age-dependent neurogenesis and neuron numbers within the olfactory bulb and hippocampus of homing pigeons. *Frontiers in Behavioral Neuroscience, 10*, 126. https://doi.org/10.3389/fnbeh.2016.00126.
Ming, G. L., & Song, H. (2005). Adult neurogenesis in the mammalian central nervous system. *Annual Review of Neuroscience, 28*, 223–250.
Ming, G. L., & Song, H. (2011). Adult neurogenesis in the mammalian brain: Significant answers and significant questions. *Neuron, 70*, 687–702. https://doi.org/10.1016/j.neuron.2011.05.001.
Moldovan, G. L., Pfander, B., & Jentsch, S. (2007). PCNA, the maestro of the replication fork. *Cell, 129*, 665–679. https://doi.org/10.1016/j.cell.2007.05.003.
Montagnese, C. M., Székely, A. D., Adám, A., & Csillag, A. (2004). Efferent connections of septal nuclei of the domestic chick (Gallus domesticus): an anterograde pathway tracing study with a bearing on functional circuits. *Journal of Comparative Neurology, 469*, 437–456.
Montagnese, C. M., Zachar, G., Bálint, E., & Csillag, A. (2008). Afferent connections of septal nuclei of the domestic chick (Gallus domesticus): A retrograde pathway tracing study. *Journal of Comparative Neurology, 511*, 109–150.
Montiel, J. F., Vasistha, N. A., Garcia-Moreno, F., & Molnar, Z. (2016). From sauropsids to mammals and back: New approaches to comparative cortical development. *Journal of Comparative Neurology, 524*, 630–645.
Nomura, T., & Hirata, T. (2017). The neocortical homologues in nonmammalian amniotes: Bridging the hierarchical concepts of homology through comparative neurogenesis. *Evolution of Nervous Systems, 2nd ed., 2*, 195–204. https://doi.org/10.1016/B978-0-12-804042-3.00041-5.

Nomura, T., Takahashi, M., Hara, Y., & Osumi, N. (2008). Patterns of neurogenesis and amplitude of Reelin expression are essential for making a mammalian-type cortex. *PLoS One, 3*, e1454. https://doi.org/10.1371/journal.pone.0001454.

O'Leary, O. F., & Cryan, J. F. (2014). A ventral view on antidepressant action: Roles for adult hippocampal neurogenesis along the dorsoventral axis. *Trends in Pharmacological Sciences, 35*, 675–687. https://doi.org/10.1016/j.tips.2014.09.011.

Ohara, S., Sato, S., Tsutsui, K.-I., Witter, M. P., & Iijima, T. (2013). Organization of multisynaptic inputs to the dorsal and ventral dentate gyrus: Retrograde trans-synaptic tracing with rabies virus vector in the rat. *PLoS One, 8*, e78928. https://doi.org/10.1371/journal.pone.0078928.

Olkowicz, S., Kocourek, M., Lučan, R. K., Porteš, M., Fitch, W. T., Herculano-Houzel, S., et al. (2016). Birds have primate-like numbers of neurons in the forebrain. *Proceedings of the National Academy of Sciences of the United States of America, 113*, 7255–7260. https://doi.org/10.1073/pnas.1517131113.

Pakhomova, A. S. (1981). Diencephalic afferents of the rat hippocampus. *Journal of Neurophysiology, 13*, 267–273.

Patel, S. N., Clayton, N. S., & Krebs, J. R. (1997). Spatial learning induces neurogenesis in the avian brain. *Behavioural Brain Research, 89*, 115–128.

Patzke, N., Manns, M., & Güntürkün, O. (2011). Telencephalic organization of the olfactory system in homing pigeons (Columba livia). *Neuroscience, 194*, 53–61. https://doi.org/10.1016/j.neuroscience.2011.08.001.

Pitkänen, A., Pikkarainen, M., Nurminen, N., & Ylinen, A. (2000). Reciprocal connections between the amygdala and the hippocampal formation, perirhinal cortex, and postrhinal cortex in rat. A review. *Annals of the New York Academy of Sciences, 911*, 369–391.

Puelles, L. (2001). Thoughts on the development, structure and evolution of the mammalian and avian telencephalic pallium. *Philosophical Transactions of the Royal Society of London. Series B, Biological sciences, 356*, 1583–1598.

Puelles, L. (2011). Pallio-pallial tangential migrations and growth signaling: New scenario for cortical evolution? *Brain, Behavior and Evolution, 78*, 108–127.

Reckfort, J. (2015). *New approaches to the interpretation of 3D-polarized light imaging signals for an advanced extraction of fiber orientation* (PhD thesis). Germany: Bergische Universität Wuppertal.

Reiner, A., Perkel, D. J., Bruce, L. L., Butler, A. B., Csillag, A., Kuenzel, W., et al.Avian Brain Nomenclature F. (2004). Revised nomenclature for avian telencephalon and some related brainstem nuclei. *Journal of Comparative Neurology, 473*, 377–414.

Robertson, B.-A., Rathbone, L., Cirillo, G., D'Eath, R. B., Bateson, M., Boswell, T., et al. (2017). Food restriction reduces neurogenesis in the avian hippocampal formation. *PLoS One, 12*, e0189158. https://doi.org/10.1371/journal.pone.0189158.

Roberts, A. C., Tomic, D. L., Parkinson, C. H., Roeling, T. A., Cutter, D. J., Robbins, T. W., et al. (2007). Forebrain connectivity of the prefrontal cortex in the marmoset monkey (Callithrix jacchus): An anterograde and retrograde tract-tracing study. *Journal of Comparative Neurology, 502*, 86–112.

Rowe, T. B., & Shepherd, G. M. (2016). Role of ortho-retronasal olfaction in mammalian cortical evolution. *Journal of Comparative Neurology, 524*, 471–495. https://doi.org/10.1002/cne.23802.

Scholzen, T., & Gerdes, J. (2000). The Ki-67 protein: From the known and the unknown. *Journal of Cellular Physiology, 182*, 311–322.

Schubert, N., Axer, M., Schober, M., Huynh, A. M., Huysegoms, M., Palomero-Gallagher, N., et al. (2016). 3D reconstructed cyto-, muscarinic M2 receptor, and fiber architecture of the rat brain registered to the Waxholm Space atlas. *Frontiers in Neuroanatomy, 10*, 51. https://doi.org/10.3389/fnana.2016.00051.

Shanahan, M., Bingman, V. P., Shimizu, T., Wild, M., & Güntürkün, O. (2013). Large-scale network organization in the avian forebrain: A connectivity matrix and theoretical analysis. *Frontiers in Computational Neuroscience, 7*, 89.

Shepherd, G. M., & Rowe, T. B. (2017). Neocortical lamination: Insights from neuron types and evolutionary precursors. *Frontiers in Neuroanatomy, 11*, 100. https://doi.org/10.3389/fnana.2017.00100.

Sherry, D. F., Grella, S. L., Guigueno, M. F., White, D. J., & Marrone, D. F. (2017). Are there place cells in the avian hippocampus? *Brain, Behavior and Evolution, 90*, 73–80. https://doi.org/10.1159/000477085.

Sherry, D. F., & Hoshooley, J. S. (2010). Seasonal hippocampal plasticity in food-storing birds. *Philosophical Transactions of the Royal Society of London. Series B, Biological sciences, 365*, 933–943. https://doi.org/10.1098/rstb.2009.0220.

Sherry, D. F., & MacDougall-Shackleton, S. A. (2015). Seasonal change in the avian hippocampus. *Frontiers in Neuroendocrinology, 37*, 158–167. https://doi.org/10.1016/j.yfrne.2014.11.008.

Silverman, A. J., Hoffmann, A. J., & Zimmermann, E. A. (1981). The descending afferent connections of the paraventricular nucleus of the hypothalamus (PVN). *Brain Research Bulletin, 6*, 47–61.

Smulders, T. V. (2017). The avian hippocampal formation and the stress response. *Brain, Behavior and Evolution, 90*, 81–91. https://doi.org/10.1159/000477654.

Snyder, J. S., Radik, R., Wojtowicz, J. M., & Cameron, H. A. (2009). Anatomical gradients of adult neurogenesis and activity: Young neurons in the ventral dentate gyrus are activated by water maze training. *Hippocampus, 19*, 360–370.

Spampanato, J., Sullivan, R. K., Turpin, F. R., Bartlett, P. F., & Sah, P. (2012). Properties of doublecortin expressing neurons in the adult mouse dentate gyrus. *PLoS One, 7*, e41029. https://doi.org/10.1371/journal.pone.0041029.

Strange, B. A., Witter, M. P., Lein, E. D., & Moser, E. I. (2014). Functional organization of the hippocampal longitudinal axis. *Nature Reviews. Neuroscience, 15*, 655–669.

Striedter, G. F. (2005). *Principles of brain evolution*. Sunderland: Sinauer.

Striedter, G. F. (2016). Evolution of the hippocampus in reptiles and birds. *Journal of Comparative Neurology, 524*, 496–517.

Striedter, G. F., & Northcutt, R. G. (2006). Head size constrains forebrain development and evolution in ray-finned fishes. *Evolution & Development, 8*, 215–222.

Swanson, L. W., & Cowan, W. M. (1977). An autoradiographic study of the organization of the efferent connections of the hippocampal formation in the rat. *Journal of Comparative Neurology, 172*, 49–84.

Swanson, C. J., & Kalivas, P. W. (2000). Regulation of locomotor activity by metabotropic glutamate receptors in the nucleus accumbens and ventral tegmental area. *The Journal of Pharmacology and Experimental Therapeutics, 292*, 406–414.

Szekely, A. D. (1999). The avian hippocampal formation: Subdivisions and connectivity. *Behavioural Brain Research, 98*, 219–225.

Szekely, A. D., & Krebs, J. R. (1996). Efferent connectivity of the hippocampal formation of the zebra finch (Taeniopygia guttata): An anterograde pathway tracing study using Phaseolus vulgaris leucoagglutinin. *Journal of Comparative Neurology, 368*, 198–214.

Tanti, A., Rainer, Q., Minier, F., Surget, A., & Belzung, C. (2012). Differential environmental regulation of neurogenesis along the septo-temporal axis of the hippocampus. *Neuropharmacology, 63*, 374–384.

Tanti, A., Westphal, W. P., Girault, V., Brizard, B., Devers, S., Leguisquet, A. M., et al. (2013). Region-dependent and stage-specific effects of stress, environmental enrichment, and antidepressant treatment on hippocampal neurogenesis. *Hippocampus, 23*, 797–811.

Taufique, S. K. T., Prabhat, A., & Kumar, V. (2018). Constant light environment suppresses maturation and reduces complexity of new born neuron processes in the hippocampus and caudal nidopallium of a diurnal corvid: Implication for impairment of the learning and cognitive performance. *Neurobiology of Learning and Memory, 147*, 120–127. https://doi.org/10.1016/j.nlm.2017.12.001.

Thierry, A. M., Gioanni, Y., Degenetais, E., & Glowinski, J. (2000). Hippocampo-prefrontal cortex pathway: Anatomical and electrophysiological characteristics. *Hippocampus, 10*, 411–419.

Thompson, C. L., Pathak, S. D., Jeromin, A., Ng, L. L., MacPherson, C. R., Mortrud, M. T., et al. (2008). Genomic anatomy of the hippocampus. *Neuron, 60*, 1010–1021. https://doi.org/10.1016/j.neuron.2008.12.008.

Tosches, M. A., Yamawaki, T. M., Naumann, R. K., Jacobi, A. A., Tushev, G., & Laurent, G. (2018). Evolution of pallium, hippocampus, and cortical cell types revealed by single-cell transcriptomics in reptiles. *Science, 360*, 881–888. https://doi.org/10.1126/science.aar4237.

Ulinski, P. S. (1983). *Dorsal ventricular ridge: Treatise on forebrain organization in reptiles and birds (Neurobiology)*. John Wiley & Sons Inc.

Wada, H., Newman, A. E., Hall, Z. J., Soma, K. K., & MacDougall-Shackleton, S. A. (2014). Effects of corticosterone and DHEA on doublecortin immunoreactivity in the song control system and hippocampus of adult song sparrows. *Developmental Neurobiology, 74*, 52–62. https://doi.org/10.1002/dneu.22132.

Walker, D. L., Miles, L. A., & Davis, M. (2009). Selective participation of the bed nucleus of the stria terminalis and CRF in sustained anxiety-like versus phasic fear-like responses. *Progress in Neuro-psychopharmacology & Biological Psychiatry, 33*, 1291–1308.

Wilson, C. L., Isokawa, M., Babb, T. L., Crandall, P. H., Levesque, M. F., & Engel, J., Jr. (1991). Functional connections in the human temporal lobe. II. Evidence for a loss of functional linkage between contralateral limbic structures. *Experimental Brain Research, 85*, 174–187.

Witter, M. P., & Amaral, D. G. (2004). Hippocampal formation. In G. Paxinos (Ed.), *The rat nervous system* (pp. 635–704). Amsterdam: Elsevier.

Witter, M. P., Kleven, H., & Kobro Flatmoen, A. (2017). Comparative contemplations on the hippocampus. *Brain, Behavior and Evolution, 90*, 15–24. https://doi.org/10.1159/000475703.

Yassa, M. A., & Stark, C. E. L. (2011). Pattern separation in the hippocampus. *Trends in Neurosciences, 34*, 515–525. https://doi.org/10.1016/j.tins.2011.06.006.

Zeineh, M. M., Palomero-Gallagher, N., Axer, M., Gräßel, D., Goubran, M., Wree, A., et al. (2017). Direct visualization and mapping of the spatial course of fiber tracts at microscopic resolution in the human hippocampus. *Cerebral Cortex, 27*, 1779–1794. https://doi.org/10.1093/cercor/bhw010.

Zheng, J., Jiang, Y. Y., Xu, L. C., Ma, L. Y., Liu, F. Y., Cui, S., et al. (2017). Adult hippocampal neurogenesis along the dorsoventral axis contributes differentially to environmental enrichment combined with voluntary exercise in alleviating chronic inflammatory pain in mice. *The Journal of Neuroscience: the Official Journal of the Society for Neuroscience, 37*, 4145–4157. https://doi.org/10.1523/JNEUROSCI.3333-16.2017.

Zilles, K., Palomero-Gallagher, N., Gräßel, D., Schlömer, P., Cremer, M., Woods, R., et al. (2016). High-resolution fiber and fiber tract imaging using polarized light microscopy in the human, monkey, rat, and mouse brain. In K. S. Rockland (Ed.), *Axons and brain architecture (2016)* (pp. 369–389). London: Elsevier.